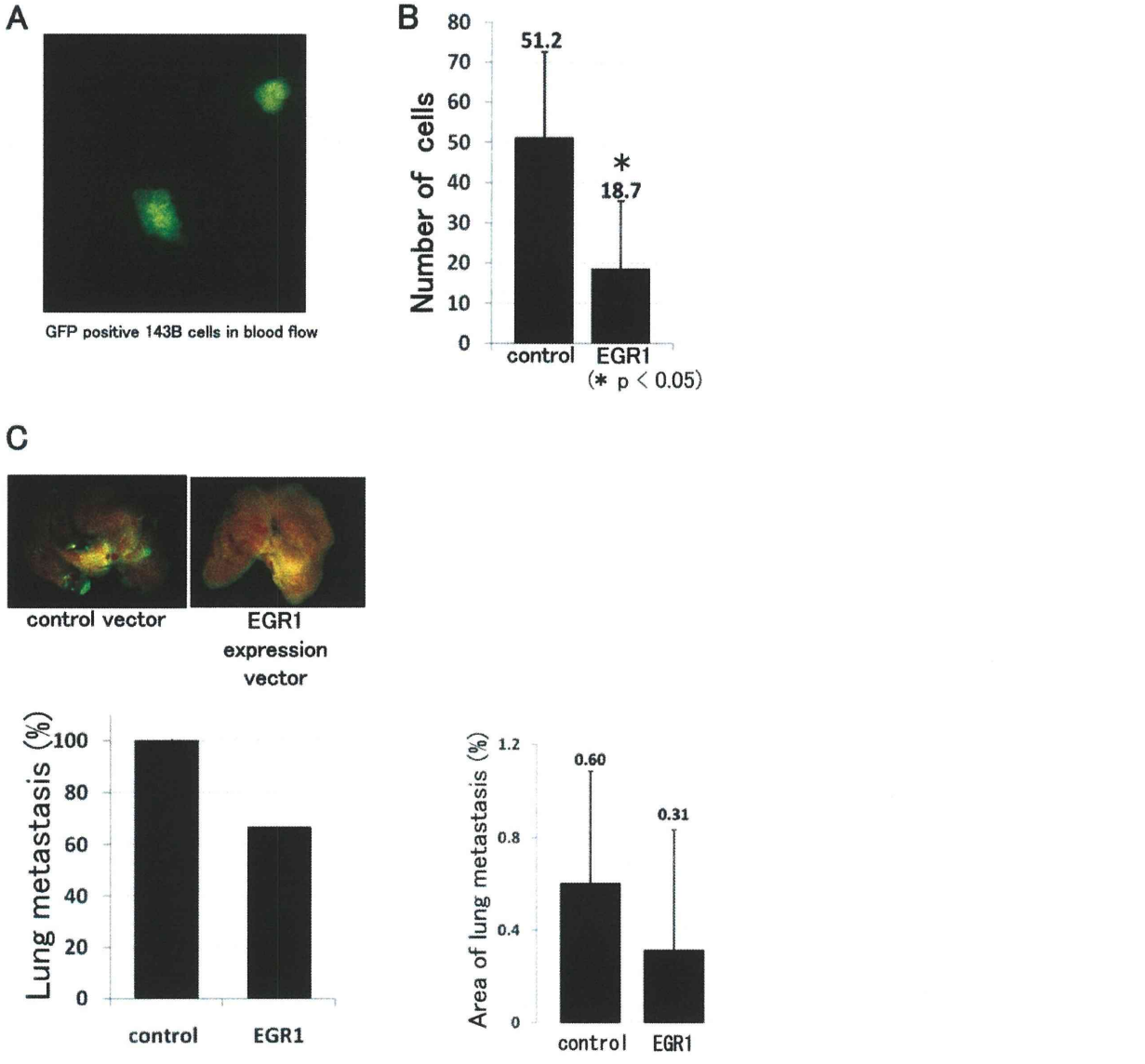

Figure 7. EGR1 prevents osteosarcoma cell migration into blood vessel in vivo. GFP expression virus-transfected 143B cells were inoculated into the knee joint. To examine tumour cell invasion of blood vessels, we counted GFP- positive- 143B cells within 50 μl blood aspirates from hearts at 5 weeks after inoculation (A). The number of GFP- positive cells in blood was decreased in EGR1 -expressing 143B- inoculated mice (B) [error bars represent mean (SD)] ($P<0.05$). Metastatic nodules in lungs were evaluated under fluorescence microscopy. Six of 6 control cell-inoculated mice exhibited lung metastases. Four of six (66.7%) EGR1-expressing cell-inoculated mice exhibited lung metastases. The percent of lung metastasis area was calculated by Lumina Vision (C).
doi:10.1371/journal.pone.0016234.g007

These findings showed that one-third of osteosarcoma patients are even poor responders to chemotherapy. Even though chemotherapy is quite benefit for osteosarcoma patients, administration of preoperative chemotherapy results in delay of surgical resection of primary tumor. It is possible that new lung metastases will develop during preoperative chemotherapy in poor or non-responders. We showed that low-dose anti-tumor agent treatment up-regulated EGR1 expression and that EGR1 prevented osteosarcoma invasion via uPA/uPAR down-regulation. These findings suggest that preoperative chemotherapy prevents the development of new lung metastases in poor or non-responders. In addition, osteosarcoma incidence rates in the United States peak in adolescence and in the elderly [23]. Many elderly patients cannot tolerate aggressive chemotherapy. Our findings suggest that low-dose chemotherapy might be useful for elderly osteosarcoma patients by preventing new metastasis when used in combination with radiation therapy or as maintenance therapy.

EGR1 has received much attention recently because of its wide range of activities as a transcription factor. Remarkably, EGR1 can exert effects as either a growth promoter or a tumor suppressor. EGR1 may induce or suppress cell proliferation or induce apoptosis of cancer cells [10,16,24–27]. Our MTT assay

and colony formation assay showed that EGR1 over-expression had no effect on osteosarcoma cell growth. Our findings suggest that the expression of EGR does not have general effects on growth and instead exerts regulatory effects that appear to be cell-type-specific.

We showed up-regulation of EGR1 following cisplatin, methotrexate, etoposide, or doxorubicin treatment, each of which exerts cytotoxic effects by different pharmacological mechanisms. EGR1 can be rapidly induced by many stimuli, including growth factors, cytokines, ultraviolet light, anti-tumour agents, and various stresses [8,10,24, Cao, 1992 #88,25,28–35]. The distinct types of stress caused by anti-tumor drugs might promote up-regulation of EGR1, although anti-tumor drugs exert different pathways. Further, we examined which signaling pathway promotes EGR1 expression following anti-tumor agent treatment. We treated osteosarcoma cell lines with anti-tumor agent and some specific inhibitors including ERK inhibitor, HIF1-α inhibitor, JAK2 inhibitor, LY294002, and others but we were unable to inhibit EGR1 expression effectively. Further examination for regulation mechanisms of EGR1 expression is needed.

The principle mode of action of doxorubicin, an anthracycline antibiotic, appears to be its ability to cross-link DNA and RNA, thereby affecting DNA and RNA synthesis [36,37]. However, recent studies have demonstrated that genotoxic (*i.e.*, DNA damaging) agents, including many important cancer chemotherapy drugs, can have significant and selective effects on the expression of certain inducible genes [38]. It has also been demonstrated that noncytotoxic doses of the DNA cross-linking cancer chemotherapy drugs MMC, cisplatin, and carboplatin were effective at significantly altering the expression of the *MDR1* gene coding for the multidrug resistance protein P-glycoprotein [37]. We were therefore interested in whether chemotherapy agents might similarly alter the expression of inducible invasion-related genes, and thereby potentially alter tumor invasiveness, and found that anti-tumour agents increased the expression of EGR1, and EGR1 decreased that of uPA and uPAR.

The uPA system is thought to play roles in several different processes important to tumor progression including angiogenesis, tumor growth, and metastasis [39]. Expression of uPA and uPAR frequently indicates a poor prognosis, and is in some cases predictive of invasion and metastasis. uPAR is also thought to play roles in the growth and metastasis of human osteosarcoma [40–44]. We showed that forced expression of EGR1 inhibited expression of uPA and uPAR. In addition, EGR1 decreased the activity of uPA. These findings suggest that up-regulation of EGR1 following chemotherapy inhibits osteosarcoma migration via uPA system. Many signaling pathways activate transcription factors that act on the uPAR promoter, driving uPAR expression in cancer [45]. uPAR transcription is controlled by ERK through activator protein 1 transcription factors [46]. Hypoxia-inducible factor 1α drive uPAR expression through a hypoxia responsive element in the uPAR promoter [47]. Nuclear factor-κB also activates uPAR expression [48]. Thus, multiple signaling inputs can up-regulate uPAR transcription in tumors. We could not detect the pathways that promote down-regulation of uPA/uPAR. Further examination for regulation mechanisms of uPA/uPAR system is needed.

Recently, many molecular target drugs have been developed [49–52]. In addition, several Notch signal inhibitors have been tested as molecular target drugs [53–55]. We previously reported that activation of Notch signaling promotes the progression of human osteosarcoma [56]. We examined the EGR1 expression by γ-secretase inhibitor, a pharmacological agent known to effectively block Notch activation. EGR1 was up-regulated by γ-secretase inhibitor in human osteosarcoma cell lines (data not shown). These findings suggest that EGR1 expression will also be up-regulated by molecular target drugs.

In summary, anti-tumor agents increased the expression of EGR1, and EGR1 decreased osteosarcoma invasion. Our findings suggest that even though chemotherapy could not prevent osteosarcoma growth in chemotherapy poor responders, chemotherapy prevents osteosarcoma cell migration into blood vessel by down-regulation of urokinase plasminogen activation via up-regulation of EGR1 during chemotherapy periods.

Supporting Information

Figure S1 Anti-tumor agent treatment increased the expression of *EGR1*. Following 48 h or 5 days drug treatments, total RNA extracted from osteosarcoma cell lines were analyzed by real-time PCR. Following 48 h treatment, cisplatin, methotrexate, etoposide or doxorubicin increased *EGR1* expression in 143B cell and Saos-2 cells. Following 5 days treatment, cisplatin increased *EGR1* expression in 143B cell. Following 5 days treatment, etoposide or doxorubicin increased *EGR1* expression in Saos-2 cells. The comparative Ct (ΔΔCt) method was used to determine fold change in expression using *GAPDH* or *ACTB*. Experiments were performed in triplicate with similar results [error bars represent mean (SD)].
(TIF)

Figure S2 Chemotherapy increased *EGR1* expression. Total RNA extracted from osteosarcoma patients' biopsy specimens and excised tumors following chemotherapy were used for real-time PCR. Real-time PCR revealed that 3 of 3 excised specimens of osteosarcoma increased *EGR1* expression 7.87- to 1.73-fold (A). One day after 4 μg doxorubicin treatment, RNA was extracted from tumor in nude mice xenograft models. Real-time PCR revealed that low dose chemotherapy increased *EGR1* expression in vivo (B) ($P<0.05$). The comparative Ct (ΔΔCt) method was used to determine fold change in expression. These experiments were performed in triplicate with similar results [error bars represent mean (SD)].
(TIF)

Figure S3 Forced expression of EGR1 does not affect osteosarcoma cell growth in vitro. We transfected control vector or EGR1 expression vector, and examined osteosarcoma cell growth. MTT assay revealed that growth of viable 143B, Saos-2, and HOS cells over 8 days was not affected by forced expression of EGR1 (A). These experiments were performed in triplicate with similar results [error bars represent mean (SD)]. Colony formation assay revealed that forced expression of EGR1 did not affect the number of colonies in soft agar (B). These experiments were performed in triplicate with similar results [error bars represent mean (SD)].
(TIF)

Figure S4 Forced expression of EGR1 decreased the expression of uPA and uPAR. Cell lysate were prepared from control vector or EGR1 expression vector stably transfected cells. ELISA assay showed that forced expression of EGR1 decreased the expression of uPA and uPAR proteins in 143B ($P<0.05$) (A). The expression of uPA and uPAR decreased in Saos-2 and HOS ($P<0.05$) (B, C). These experiments were in triplicate with similar results [error bars represent mean (SD)].
(TIF)

Figure S5 Low dose anti-tumor agent treatment decreased the expression of *uPA* and *uPAR*. Following 24 h drug treatments, total RNA extracted from osteosarcoma cell lines were analyzed by real-time PCR. Treatment with cisplatin, methotrexate, etoposide or doxorubicin decreased *uPA and uPAR* expression in 143B and Saos-2 cells ($P<0.05$). The comparative Ct ($\Delta\Delta$Ct) method was used to determine fold change in expression using *GAPDH* or *ACTB*. Experiments were performed in triplicate with similar results [error bars represent mean (SD)].
(TIF)

Figure S6 Chemotherapy prevents expression of *uPA* and *uPAR* by down-regulation of EGR1. Twenty four hours after 4 μg doxorubicin treatment, RNA was extracted from tumour in nude mice xenograft model. Real-time PCR revealed that chemotherapy decreased *uPA* and *uPAR* expression in vivo (A) ($P<0.05$). To examined whether EGR1 affects the expression of uPA and uPAR in vivo. RNA was prepared from tumor formed by control vector or EGR1 expression vector transfected cells. Real-time PCR revealed that forced expression of EGR1 decreased *uPA* and uPAR expression in vivo (B) ($P<0.05$). The comparative Ct ($\Delta\Delta$Ct) method was used to determine fold change in expression using GAPDH. These experiments were performed in triplicate with similar results [error bars represent mean (SD)].
(TIF)

Acknowledgments

We thank to Dr. Mitsuhiko Osaki (Tottori University Faculty of Medicine, Graduate School of Medical Sciences, Department of Biomedical Science, Division of Molecular Genetics and Biofunction) for developing the lung metastasis model using 143B.

Author Contributions

Conceived and designed the experiments: KI SN SK TS. Performed the experiments: YM YI TY HN. Analyzed the data: YM SK TS. Contributed reagents/materials/analysis tools: YM HN. Wrote the paper: TS.

References

1. Iwamoto Y, Tanaka K, Isu K, Kawai A, Tatezaki S, et al. (2009) Multiinstitutional phase II study of neoadjuvant chemotherapy for osteosarcoma (NECO study) in Japan: NECO-93J and NECO-95J. J Orthop Sci 14: 397–404.
2. Goorin AM, Schwartzentruber DJ, Devidas M, Gebhardt MC, Ayala AG, et al. (2003) Presurgical chemotherapy compared with immediate surgery and adjuvant chemotherapy for nonmetastatic osteosarcoma: Pediatric Oncology Group Study POG-8651. J Clin Oncol 21: 1574–1580.
3. Patel SJ, Lynch JW, Jr., Johnson T, Carroll RR, Schumacher C, et al. (2002) Dose-intense ifosfamide/doxorubicin/cisplatin based chemotherapy for osteosarcoma in adults. Am J Clin Oncol 25: 489–495.
4. Bielack SS, Kempf-Bielack B, Delling G, Exner GU, Flege S, et al. (2002) Prognostic factors in high-grade osteosarcoma of the extremities or trunk: an analysis of 1,702 patients treated on neoadjuvant cooperative osteosarcoma study group protocols. J Clin Oncol 20: 776–790.
5. Meyers PA, Schwartz CL, Krailo M, Kleinerman ES, Betcher D, et al. (2005) Osteosarcoma: a randomized, prospective trial of the addition of ifosfamide and/or muramyl tripeptide to cisplatin, doxorubicin, and high-dose methotrexate. J Clin Oncol 23: 2004–2011.
6. Bacci G, Forni C, Longhi A, Ferrari S, Mercuri M, et al. (2007) Local recurrence and local control of non-metastatic osteosarcoma of the extremities: a 27-year experience in a single institution. J Surg Oncol 96: 118–123.
7. Lewis IJ, Nooij MA, Whelan J, Sydes MR, Grimer R, et al. (2007) Improvement in histologic response but not survival in osteosarcoma patients treated with intensified chemotherapy: a randomized phase III trial of the European Osteosarcoma Intergroup. J Natl Cancer Inst 99: 112–128.
8. Back SJ, Kim JS, Moore SM, Lee SH, Martinez J, et al. (2005) Cyclooxygenase inhibitors induce the expression of the tumor suppressor gene EGR-1, which results in the up-regulation of NAG-1, an antitumorigenic protein. Mol Pharmacol 67: 356–364.
9. Levin WJ, Press MF, Gaynor RB, Sukhatme VP, Boone TC, et al. (1995) Expression patterns of immediate early transcription factors in human non-small cell lung cancer. The Lung Cancer Study Group. Oncogene 11: 1261–1269.
10. Huang RP, Fan Y, de Belle I, Niemeyer C, Gottardis MM, et al. (1997) Decreased Egr-1 expression in human, mouse and rat mammary cells and tissues correlates with tumor formation. Int J Cancer 72: 102–109.
11. Huang RP, Liu C, Fan Y, Mercola D, Adamson ED (1995) Egr-1 negatively regulates human tumor cell growth via the DNA-binding domain. Cancer Res 55: 5054–5062.
12. Hotta T, Motoyama T, Watanabe H (1992) Three human osteosarcoma cell lines exhibiting different phenotypic expressions. Acta Pathol Jpn 42: 595–603.
13. Sasaki H, Setoguchi T, Matsunoshita Y, Gao H, Hirotsu M, et al. (2010) The knock-down of overexpressed EZH2 and BMI-1 does not prevent osteosarcoma growth. Oncol Rep 23: 677–684.
14. Hirotsu M, Setoguchi T, Sasaki H, Matsunoshita Y, Gao H, et al. (2010) Smoothened as a new therapeutic target for human osteosarcoma. Mol Cancer 9: 5.
15. Hirotsu M, Setoguchi T, Matsunoshita Y, Sasaki H, Nagao H, et al. (2009) Tumour formation by single fibroblast growth factor receptor 3-positive rhabdomyosarcoma-initiating cells. Br J Cancer 101: 2030–2037.
16. de Belle I, Huang RP, Fan Y, Liu C, Mercola D, et al. (1999) p53 and Egr-1 additively suppress transformed growth in HT1080 cells but Egr-1 counteracts p53-dependent apoptosis. Oncogene 18: 3633–3642.
17. Liu C, Yao J, Mercola D, Adamson E (2000) The transcription factor EGR-1 directly transactivates the fibronectin gene and enhances attachment of human glioblastoma cell line U251. J Biol Chem 275: 20315–20323.
18. Shingu T, Bornstein P (1994) Overlapping Egr-1 and Sp1 sites function in the regulation of transcription of the mouse thrombospondin 1 gene. J Biol Chem 269: 32551–32557.
19. Rao JS (2003) Molecular mechanisms of glioma invasiveness: the role of proteases. Nat Rev Cancer 3: 489–501.
20. Wittig JC, Bickels J, Priebat D, Jelinek J, Kellar-Graney K, et al. (2002) Osteosarcoma: a multidisciplinary approach to diagnosis and treatment. Am Fam Physician 65: 1123–1132.
21. Ta HT, Dass CR, Choong PF, Dunstan DE (2009) Osteosarcoma treatment: state of the art. Cancer Metastasis Rev 28: 247–263.
22. Bacci G, Longhi A, Fagioli F, Briccoli A, Versari M, et al. (2005) Adjuvant and neoadjuvant chemotherapy for osteosarcoma of the extremities: 27 year experience at Rizzoli Institute, Italy. Eur J Cancer 41: 2836–2845.
23. Mirabello L, Troisi RJ, Savage SA (2009) International osteosarcoma incidence patterns in children and adolescents, middle ages and elderly persons. Int J Cancer 125: 229–234.
24. Yu J, Zhang SS, Saito K, Williams S, Arimura Y, et al. (2009) PTEN regulation by Akt-EGR1-ARF-PTEN axis. Embo J 28: 21–33.
25. Kim J, Lee YH, Kwon TK, Chang JS, Chung KC, et al. (2006) Phospholipase D prevents etoposide-induced apoptosis by inhibiting the expression of early growth response-1 and phosphatase and tensin homologue deleted on chromosome 10. Cancer Res 66: 784–793.
26. Baron V, Adamson ED, Calogero A, Ragona G, Mercola D (2006) The transcription factor Egr1 is a direct regulator of multiple tumor suppressors including TGFbeta1, PTEN, p53, and fibronectin. Cancer Gene Ther 13: 115–124.
27. Mahalingam D, Natoni A, Keane M, Samali A, Szegezdi E (2010) Early growth response-1 is a regulator of DR5-induced apoptosis in colon cancer cells. Br J Cancer 102: 754–764.
28. Chen CC, Lee WR, Safe S (2004) Egr-1 is activated by 17beta-estradiol in MCF-7 cells by mitogen-activated protein kinase-dependent phosphorylation of ELK-1. J Cell Biochem 93: 1063–1074.
29. Quinones A, Dobberstein KU, Rainov NG (2003) The egr-1 gene is induced by DNA-damaging agents and non-genotoxic drugs in both normal and neoplastic human cells. Life Sci 72: 2975–2992.
30. Liu X, Kelm RJ Jr., Strauch AR (2009) Transforming growth factor beta1-mediated activation of the smooth muscle alpha-actin gene in human pulmonary myofibroblasts is inhibited by tumor necrosis factor-alpha via mitogen-activated protein kinase kinase 1-dependent induction of the Egr-1 transcriptional repressor. Mol Biol Cell 20: 2174–2185.
31. Lim CP, Jain N, Cao X (1998) Stress-induced immediate-early gene, egr-1, involves activation of p38/JNK1. Oncogene 16: 2915–2926.
32. Santiago FS, Lowe HC, Day FL, Chesterman CN, Khachigian LM (1999) Early growth response factor-1 induction by injury is triggered by release and paracrine activation by fibroblast growth factor-2. Am J Pathol 154: 937–944.
33. Schwachtgen JL, Houston P, Campbell C, Sukhatme V, Braddock M (1998) Fluid shear stress activation of egr-1 transcription in cultured human endothelial and epithelial cells is mediated via the extracellular signal-related kinase 1/2 mitogen-activated protein kinase pathway. J Clin Invest 101: 2540–2549.
34. Chang Y, Lee HH, Chen YT, Lu J, Wu SY, et al. (2006) Induction of the early growth response 1 gene by Epstein-Barr virus lytic transactivator Zta. J Virol 80: 7748–7755.
35. Su L, Cheng H, Sampaio AV, Nielsen TO, Underhill TM (2010) EGR1 reactivation by histone deacetylase inhibitors promotes synovial sarcoma cell death through the PTEN tumor suppressor. Oncogene 29: 4352–4361.

36. Gottesman MM, Pastan I (1993) Biochemistry of multidrug resistance mediated by the multidrug transporter. Annu Rev Biochem 62: 385–427.
37. Ihnat MA, Lariviere JP, Warren AJ, La Ronde N, Blaxall JR, et al. (1997) Suppression of P-glycoprotein expression and multidrug resistance by DNA cross-linking agents. Clin Cancer Res 3: 1339–1346.
38. Hamilton JW, McCaffrey J, Caron RM, Louis CA, Treadwell MD, et al. (1994) Genotoxic chemical carcinogens target inducible genes in vivo. Ann N Y Acad Sci 726: 343–345.
39. Mazar AP (2008) Urokinase plasminogen activator receptor choreographs multiple ligand interactions: implications for tumor progression and therapy. Clin Cancer Res 14: 5649–5655.
40. Kariko K, Kuo A, Boyd D, Okada SS, Cines DB, et al. (1993) Overexpression of urokinase receptor increases matrix invasion without altering cell migration in a human osteosarcoma cell line. Cancer Res 53: 3109–3117.
41. MacEwen EG, Kutzke J, Carew J, Pastor J, Schmidt JA, et al. (2003) c-Met tyrosine kinase receptor expression and function in human and canine osteosarcoma cells. Clin Exp Metastasis 20: 421–430.
42. MacEwen EG, Pastor J, Kutzke J, Tsan R, Kurzman ID, et al. (2004) IGF-1 receptor contributes to the malignant phenotype in human and canine osteosarcoma. J Cell Biochem 92: 77–91.
43. de Bock CE, Lin Z, Itoh T, Morris D, Murrell G, et al. (2005) Inhibition of urokinase receptor gene expression and cell invasion by anti-uPAR DNAzymes in osteosarcoma cells. Febs J 272: 3572–3582.
44. Dass CR, Nadesapillai AP, Robin D, Howard ML, Fisher JL, et al. (2005) Downregulation of uPAR confirms link in growth and metastasis of osteosarcoma. Clin Exp Metastasis 22: 643–652.
45. Smith HW, Marshall CJ (2010) Regulation of cell signalling by uPAR. Nat Rev Mol Cell Biol 11: 23–36.
46. Lengyel E, Wang H, Stepp E, Juarez J, Wang Y, et al. (1996) Requirement of an upstream AP-1 motif for the constitutive and phorbol ester-inducible expression of the urokinase-type plasminogen activator receptor gene. J Biol Chem 271: 23176–23184.
47. Krishnamachary B, Berg-Dixon S, Kelly B, Agani F, Feldser D, et al. (2003) Regulation of colon carcinoma cell invasion by hypoxia-inducible factor 1. Cancer Res 63: 1138–1143.
48. Rius J, Guma M, Schachtrup C, Akassoglou K, Zinkernagel AS, et al. (2008) NF-kappaB links innate immunity to the hypoxic response through transcriptional regulation of HIF-1alpha. Nature 453: 807–811.
49. Mahalingam D, Mita A, Sankhala K, Swords R, Kelly K, et al. (2009) Targeting sarcomas: novel biological agents and future perspectives. Curr Drug Targets 10: 937–949.
50. Lammers T, Hennink WE, Storm G (2008) Tumour-targeted nanomedicines: principles and practice. Br J Cancer 99: 392–397.
51. Knight ZA, Lin H, Shokat KM (2010) Targeting the cancer kinome through polypharmacology. Nat Rev Cancer 10: 130–137.
52. Zhang J, Yang PL, Gray NS (2009) Targeting cancer with small molecule kinase inhibitors. Nat Rev Cancer 9: 28–39.
53. Henley DB, May PC, Dean RA, Siemers ER (2009) Development of semagacestat (LY450139), a functional gamma-secretase inhibitor, for the treatment of Alzheimer's disease. Expert Opin Pharmacother 10: 1657–1664.
54. Bateman RJ, Siemers ER, Mawuenyega KG, Wen G, Browning KR, et al. (2009) A gamma-secretase inhibitor decreases amyloid-beta production in the central nervous system. Ann Neurol 66: 48–54.
55. Fleisher AS, Raman R, Siemers ER, Becerra L, Clark CM, et al. (2008) Phase 2 safety trial targeting amyloid beta production with a gamma-secretase inhibitor in Alzheimer disease. Arch Neurol 65: 1031–1038.
56. Tanaka M, Setoguchi T, Hirotsu M, Gao H, Sasaki H, et al. (2009) Inhibition of Notch pathway prevents osteosarcoma growth by cell cycle regulation. Br J Cancer 100: 1957–1965.

Journal of Pathology
J Pathol 2011; 224: 169–179
Published online in Wiley Online Library
(wileyonlinelibrary.com) DOI: 10.1002/path.2880

ORIGINAL PAPER

Role of GLI2 in the growth of human osteosarcoma

Hiroko Nagao,[1] Kosei Ijiri,[1] Masataka Hirotsu,[1] Yasuhiro Ishidou,[2] Takuya Yamamoto,[1] Satoshi Nagano,[1] Takumi Takizawa,[3] Kinichi Nakashima,[3] Setsuro Komiya[1] and Takao Setoguchi[1]*

[1] Department of Orthopaedic Surgery, Graduate School of Medical and Dental Sciences, Kagoshima University, Japan
[2] Department of Medical Joint Materials, Graduate School of Medical and Dental Sciences, Kagoshima University, Japan
[3] Laboratory of Molecular Neuroscience, Graduate School of Biological Sciences, Nara Institute of Science and Technology, Japan

*Correspondence to: Takao Setoguchi, Department of Orthopaedic Surgery, Graduate School of Medical and Dental Sciences, Kagoshima University, 8-35-1 Sakuragaoka, Kagoshima 890-8520, Japan. e-mail: setoro@m2.kufm.kagoshima-u.ac.jp

Abstract

The Hedgehog pathway functions as an organizer in embryonic development. Aberrant activation of the Hedgehog pathway has been reported in various types of malignant tumours. The GLI2 transcription factor is a key mediator of Hedgehog pathway but its contribution to neoplasia is poorly understood. To establish the role of GLI2 in osteosarcoma, we examined its expression by real-time PCR using biopsy tissues. To examine the function of GLI2, we evaluated the growth of osteosarcoma cells and their cell cycle after *GLI2* knockdown. To study the effect of GLI2 activation, we examined mesenchymal stem cell growth and the cell cycle after forced expression of GLI2. We found that *GLI2* was aberrantly over-expressed in human osteosarcoma biopsy specimens. *GLI2* knockdown by RNA interferences prevented osteosarcoma growth and anchorage-independent growth. Knockdown of *GLI2* promoted the arrest of osteosarcoma cells in G_1 phase and was accompanied by reduced protein expression of the cell cycle accelerators cyclin D1, SKP2 and phosphorylated Rb. On the other hand, knockdown of *GLI2* increased the expression of $p21^{cip1}$. In addition, over-expression of GLI2 promoted mesenchymal stem cell proliferation and accelerated their cell cycle progression. Finally, evaluation of mouse xenograft models showed that *GLI2* knockdown inhibited the growth of osteosarcoma in nude mice. Our findings suggest that inhibition of GLI2 may represent an effective therapeutic approach for patients with osteosarcoma.

Keywords: osteosarcoma; Hedgehog; GLI2; cell cycle

Received 1 October 2010; Revised 12 February 2011; Accepted 20 February 2011

No conflicts of interest were declared.

Introduction

Osteosarcoma is a highly malignant bone tumour and is the most commonly encountered malignant bone tumour in children and adolescents [1,2]. Furthermore, a large number of patients with osteosarcoma eventually develop pulmonary metastases and die, despite conventional multi-agent chemotherapy and surgical excision of the tumour mass [3]. The survival rate of patients treated with intensive multidrug chemotherapy and aggressive local control interventions has been reported to be 60–80% [4,5]. In patients with a high-grade osteosarcoma, the clinical detection of a metastatic disease at first diagnosis is predictive of a poor outcome, with long-term survival rates in the range 10–40% [6]. It has been reported that aberrant activation of cell cycle progression affects the pathogenesis of osteosarcoma [7]. Although inactivation of the deregulated cell cycle seems promising, the molecular mechanisms of osteosarcoma cell growth remain unclear.

Hedgehog–GLI signalling is involved in various steps of development and is induced via the Patched (PTCH1) and Smoothened (SMO) Hedgehog receptors. Activated SMOs promote the translocation of GLI zinc-finger transcription factors into the nucleus [8,9]. In mammals, three transcription factors, viz GLI1, GLI2 and GLI3, activate the transcription of Hedgehog target genes [10,11]. The transcription induced by Gli2 is crucial for development, because *Gli2* knockout mice die prenatally and show defects of the central nervous system [12]. Aberrant activation of Hedgehog pathway is associated with malignant tumours (reviewed in [13]). Our findings indicate that GLI2 is actively involved in the patho-aetiology of osteosarcoma, because suppression of GLI2 inhibits osteosarcoma growth via cell cycle regulation.

Materials and methods

Cell culture

The osteosarcoma cell lines 143B, Saos-2 and HOS were purchased from the American Type Culture Collection (ATCC; Manassas, USA). Osteosarcoma cells

were cultured in Dulbecco's modified Eagle's medium (DMEM) with 10% fetal bovine serum (FBS), penicillin (100 U/ml) and streptomycin (100 μg/ml). The human hTERT-immortalized mesenchymal stem cell line (YKNK-12) was kindly provided by Dr Kobayashi (Okayama University) [14]. YKNK-12 cells were grown in the culture medium described above. Normal human osteoblast cells (NHOsts; Sanko Junyaku, Tokyo, Japan) were grown in OBM™ medium (Cambrex, East Rutherford, NJ, USA). All cells were cultured at 37 °C in a humidified incubator containing 5% CO_2.

Biopsy samples

Human osteosarcoma biopsy tissues were collected from primary lesions before any diagnostic or therapeutic treatment. Control specimens were collected from the femoral bone of patients undergoing total hip arthroplasty. The study protocol was approved by the Review Board of Graduate School of Kagoshima University. Written informed consent was obtained from all patients.

Cell growth assay

The 3-(4,5-dimethylthiazol-2-yl)-2,5-diphenyltetrazolium bromide (MTT) assay was used to evaluate cell proliferation, as previously described [15]. Briefly, cells cultured on microplates were incubated with the MTT substrate for 4 h, and subsequently lysed. The developed optical density of the compound was then analysed using a microplate reader (Bio-Rad, Hercules, CA, USA). GANT61 was obtained from Alexis Biochemicals (CA, USA). The pCS2–MT GLI2ΔN plasmid was provided by Addgene (MA, USA). *GLI2* siRNA was purchased from Santa Cruz Biotechnology (CA, USA). An shRNA plasmid for human *GLI2* was purchased from SA Biosciences (MD, USA). *GLI2* and control shRNAs were cloned into the pGeneClip™ neomycin-resistant vector, which is under the control of the U1 promoter. Transfection of the plasmid was performed according to the supplier's recommendations, using FuGENE6 (Roche, Basel, Switzerland).

Soft agar assay

Cells were suspended in DMEM containing 0.33% soft agar and 5% FBS, and then plated on a 0.5% soft agar layer. The cells were cultured at a density of 5×10^3 cells/well in six-well plates. Fourteen days later, the number of colonies was counted. Every experiment was performed in triplicate, and all experiments were performed three times.

Real-time quantitative PCR assay

Real-time quantitative PCR assay was performed as previously described [16]. Each primer set used amplified a 150–200 bp amplicon. The miR-Vana RNA isolation kit or TRIzol (Invitrogen, Carlsbad, CA, USA) were used for total RNA purification. PCR was performed using SYBR Green as the dye for quantification (Bio-Rad) and analysed using MiniOpticon™ (Bio-Rad). The comparative Ct ($^{\Delta\Delta}$ Ct) analysis method was used to evaluate the fold change of mRNA expression, using the expression of *GAPDH* or *ACTB* as a reference. All PCR reactions were performed in triplicate. All primers were designed using Primer3 software. The following primers were used: *PTCH1*: 5′-TAACGCTGCAACAACTCAGG-3′, 5′-GAAGGCTGTGACATTGCTGA-3′; *SMO*: 5′-GGG AGGCTACTTCCTCATCC-3′, 5′-GGCAGCTGAAGG TAATGAGC-3′; *GLI2*: 5′-CGACACCAGGAAGGAA GGTA-3′, 5′-AGAACGGAGGTAGTGCTCCA-3′; *cyclin D1*: 5′-ACAAACAGATCATCCGCAAACAC-3′, 5′-TGTTGGGGCTCCTCAGGTTC-3′; *SKP2*: 5′-TGG GAATCTTTTCCTGTCTG-3′, 5′-GAACACTGAGAC AGTATGCC-3′; *GAPDH*: 5′-GAAGGTGAAGGTCG GAGTC-3′, 5′-GAAGATGGTGATGGGATTTC-3′; *ACTB*: 5′-AGAAAATCTGGCACCACACC-3′, 5′-AG AGGCGTACAGGGATAGCA-3′.

Western blotting

Cells were lysed using NP40 buffer including 0.5% NP40, 10 mM Tris–HCl, pH 7.4, 150 mM NaCl, 3 mM pAPMSF (Wako Chemicals, Kanagawa, Japan), 5 mg/ml aprotinin (Sigma, St Louis, MO, USA), 2 mM sodium orthovanadate (Wako Chemicals, Kanagawa, Japan) and 5 mM EDTA. SDS–PAGE and immunoblotting were subsequently performed and the following antibodies used: GLI2, cyclin D1, p21, SKP2, pRb and actin (Santa Cruz). The ECL reagent was used and chemiluminescence detected (Amersham, Giles, UK).

Plasmid construction

A fragment containing the GLI2ΔN region was obtained from the pCS2-MT GLI2ΔN plasmid (Addgene) and subcloned into the pcDNA3 plasmid.

Luciferase assay

8 × 3′Gli-BS–δ51LucII (GLI–Luc) and 8 × m3′Gli-BS–δ51LucII (mutant-Luc) reporter genes were kindly provided by Dr Sasaki H. [17,18]. Luciferase assays were carried out as described previously [19]. In brief, cells (1.5×10^4 cells/well) were transfected with 400 ng/well of firefly luciferase expression vectors and 1 ng/well internal control vector, pGL4.74 (Promega, Madison, WI, USA) using the FuGENE6 followed by the incubation for 24 h. Recombinant Sonic Hedgehog (R&D Systems, Minneapolis, MO, USA) was added to the well and after 24 h the activities of luciferase were measured, using the Dual-Luciferase Reporter Assay System (Promega) according to the supplier's instructions.

Animal model

Xenograft experiments were performed as previously described [20]. Briefly, control or *GLI2* shRNA-transfected 143B cells (1×10^6) were suspended in 100 µl Matrigel (BD, NJ, USA). Cell suspensions were subcutaneously inoculated in 5 week-old nude mice. Tumour size was calculated weekly, using the formula $LW^2/2$ (where L and W represent the length and width of the tumour). Mice were randomly treated with GANT61 (50 mg/kg) or an equal volume of DMSO as control. GANT61 or DMSO was also injected subcutaneously. Injection of GANT61 started 1 week after inoculation of 143B cells. Treatments with GANT61 or DMSO were performed every other day. All animal experiments were performed in compliance with the guidelines of the Institute of Laboratory Animal Sciences, Graduate School of Medical and Dental Sciences, Kagoshima University. Every effort was employed to minimize the number of animals used and animal pain.

Cell cycle analysis

Cells were harvested with trypsin–EDTA. The cells were rinsed with PBS, fixed with 70% ethanol for 2 hr at 4 °C, washed three times with cold PBS and resuspended with 500 µL staining buffer containing PBS, pH 7.4, RNase A and 50 µg/ml propidium iodide (Wako). DNA content was examined by flow cytometry, using FACS Vantage SE (Becton-Dickinson, Franklin Lakes, NJ, USA) or CyAn™ ADP (Beckman Coulter, CA, USA) with FlowJo software (Tree Star) and Summit software (Beckman Coulter), respectively.

Statistical analysis

All experiments were performed three times unkess otherwise stated, and samples were analysed in triplicate. Results are presented as mean (SD). The statistical difference between groups was assessed by applying Student's t-test for unpaired data, using Microsoft Office Excel (Microsoft, Albuquerque, NM, USA) and Statistica (StatSoft, Tulsa, OK, USA).

Results

Activation of Hedgehog pathway in human osteosarcoma

We previously reported that several genes of the Hedgehog pathway were increased in five osteosarcoma cell lines and nine osteosarcoma biopsy specimens [21]. In the present study, we examined the expression of *SMO*, *PTCH1* and *GLI2* in three additional osteosarcoma biopsy tissues. We found that *SMO* expression was up-regulated in all osteosarcoma patient tissues, from 7.3- to 183-fold (Figure 1A). Similarly, the expression of *PTCH1* and *GLI2* was up-regulated in all three biopsy samples, from 8.6- to 72.3-fold and from 1.6- to 45.6-fold, respectively (Figure 1A). In agreement with these results, recombinant Sonic Hedgehog activates a reporter gene carrying $8 \times 3'$ Gli-BS–δ51LucII (GLI–Luc) in 143B and Saos-2 human osteosarcoma cells (Figure 1B) [17,18]. These findings corroborate our previous findings and indicate that the Hedgehog pathway is active in human osteosarcoma [21].

Inhibition of GLI prevents osteosarcoma cell proliferation

To examine the effects of GLI inhibition, we used GANT61, a pharmacological agent known to effectively block GLI transcription [22]. The MTT assay revealed that GANT61 dose-dependently inhibited the proliferation of 143B, Saos-2 and HOS cells (Figure 2A–C). In contrast, the same concentration of GANT61 did not affect the proliferation of normal human osteoblasts (NHOst) (Figure 2D). These findings suggest that inhibition of GLI prevents osteosarcoma proliferation *in vitro*.

Knockdown of *GLI2* prevents osteosarcoma proliferation *in vitro*

In order to evaluate the function of GLI in osteosarcoma, we knocked down GLI expression by using siRNA; scrambled siRNA was used as a negative control. MTT assay revealed that knockdown of *GLI1* did not affect the osteosarcoma cell proliferation (data not shown). On the other hand, MTT assay showed that knockdown of *GLI2* inhibited the proliferation of 143B and Saos-2 cells (Figure 3B). To rule out the possibility of an artifact due to off-target effects, we transfected the cells with two other shRNA sequences and obtained results comparable to those observed with *GLI2* siRNA (data not shown). We next examined the effects of *GLI2* knockdown on anchorage-independent osteosarcoma growth. The colony formation assay revealed that knockdown of *GLI2* reduced the number of colonies formed in soft agar (Figure 3C). These findings revealed that *GLI2* knockdown inhibits osteosarcoma growth.

GLI2 knockdown prevents cell cycle progression of human osteosarcoma cells

We next examined the role of GLI2 in the regulation of cell cycle. In 143B cells, following *GLI2* knockdown by *GLI2* shRNA, the proportion of cells in G_1 phase increased from 74.2% to 80.4% (Figure 4A). In Saos-2 cells, following *GLI2* knockdown by *GLI2* shRNA, the proportion of cells in G_1 phase increased from 60.5% to 68.7% (see Supporting information, Figure S1A), indicating that knockdown of *GLI2* promoted cell cycle arrest. We further examined the expression of cell cycle-related genes. Real-time PCR revealed that knockdown of *GLI2* decreased the expression of cell cycle accelerators, such as *cyclin D1* and

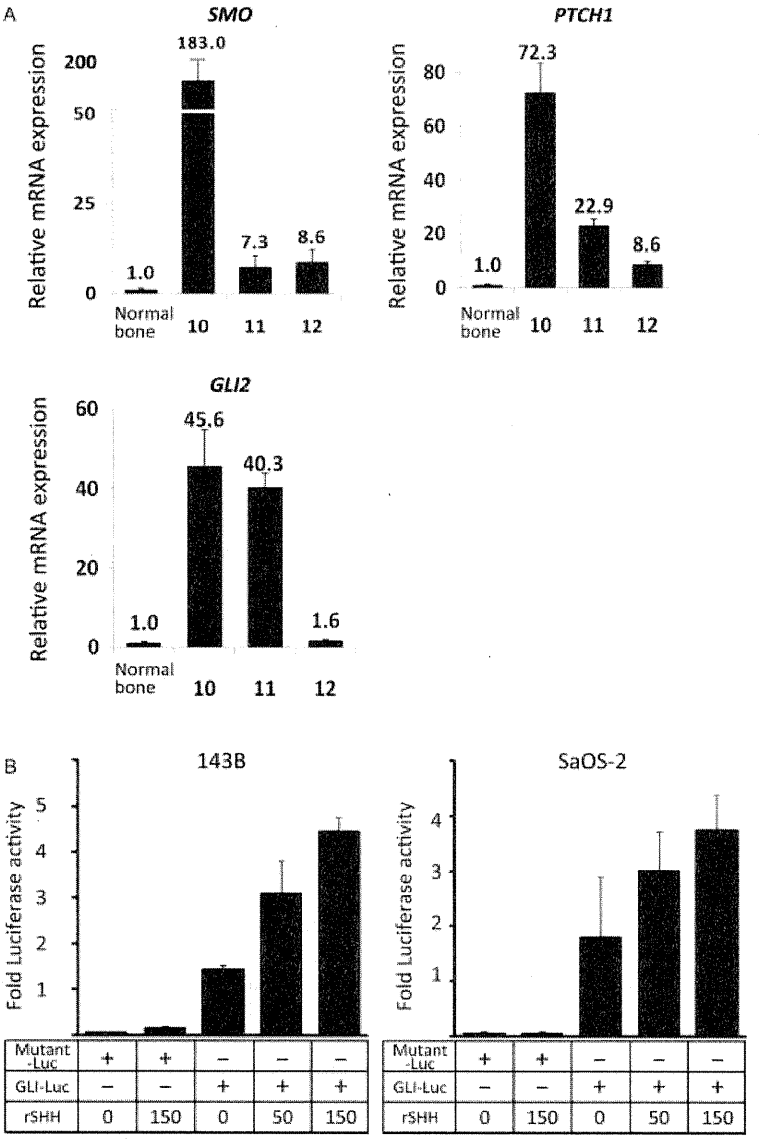

Figure 1. Activation of the Hedgehog pathway in human osteosarcoma. (A) Total RNA obtained from osteosarcoma biopsy tissues was examined by real-time quantitative PCR. Comparative Ct ($^{\Delta\Delta}$ Ct) analysis was performed to evaluate fold changes of mRNA expression using *GAPDH* or *ACTB*. All three human osteosarcoma biopsy specimens showed increased expression of *SMO* (7.3–183.0-fold), *PTCH1* (8.6–72.3-fold) and *GLI2* (1.6–45.6-fold). (B) 143B and Saos-2 cells were co-transfected with 8 × 3′ Gli-BS–δ51LucII (GLI-Luc), 8 × m3′ GLI-BS–δ51LucII (mutant-Luc) and internal control luciferase vector. The cells were treated with recombinant sonic hedgehog (rSHH). The luciferase activity was analysed after 24 h transfection and normalized to internal control luciferase activity. Values represent mean ± SD ($n = 3$).

SKP2 (Figure 4B). In mammals, cell cycle regulators are short-lived proteins that are regulated by protein degradation. Western blot analysis further confirmed that knockdown of *GLI2* decreased the protein levels of cyclin D1, pRb and SKP2 (Figure 4C). We next examined the expression of $p21^{cip1}$, a negative regulator of cell cycle progression. Western blot analysis revealed that $p21^{cip1}$ was up-regulated following knockdown of *GLI2* (Figure 4C). Taken together, these findings indicate that knockdown of *GLI2* promoted cell cycle arrest in G_1 phase by inhibiting the progression of the cycle from G_1 to S phase.

Over-expression of GLI2 accelerates mesenchymal stem cell proliferation

To examine the role of GLI2 in the pathogenesis of osteosarcoma, we over-expressed GLI2. Although the origin of osteosarcoma is still controversial, it is believed that it originates from osteoblasts or mesenchymal stem cells [23]. In this regard, we studied the effects of GLI2 over-expression in the immortalized human mesenchymal stem cell line (YKNK-12) [14]. We assessed the proliferation of YKNK-12 cells following transfection with the GLI2ΔN expression vector, which exhibits potent transcriptional activity *in vivo* [24]. The MTT assay showed that forced

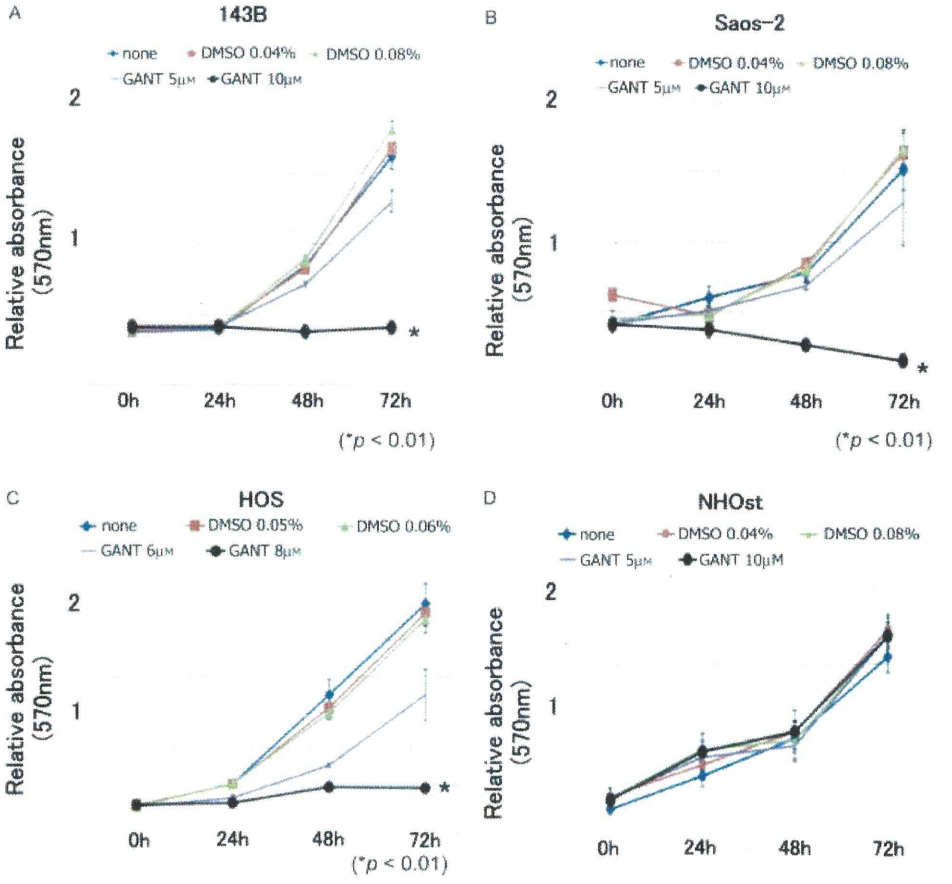

Figure 2. Inhibition of GLI prevents osteosarcoma cells proliferation. (A–C) GANT61 dose-dependently inhibited the growth of 143B, Saos-2 and HOS cells at 72 h ($*p < 0.01$). (D) At the same time point, GANT61 did not affect the growth of normal osteoblast cells (NHOst) ($n > 3$; error bars indicate SD).

expression of GLI2ΔN promoted YKNK-12 proliferation to a greater extent than transfection with control vector (Figure 5B). These findings suggest that GLI2 promotes mesenchymal stem cell proliferation. We also examined the role of GLI2 in regulating cell cycle in mesenchymal stem cells. Following forced expression of GLI2ΔN, 62.9% of the cells were in G_1 phase, 12.5% were in S phase and 22.9% were in the G_2–M phase, whereas 72.0%, 9.8% and 17.0% of cells were in G_1, S and G_2–M phases, respectively, following transfection with the control vector (Figure 5C). These findings suggest that GLI2 accelerates cell cycle progression of mesenchymal stem cells.

GLI2 knockdown inhibits osteosarcoma growth in nude mice

To confirm the role of *GLI2* knockdown in osteosarcoma growth, we tested the effects of *GLI2* knockdown in nude mice. Inoculation of 143B cells, previously transfected with *GLI2* shRNA, resulted in a statistically significant reduction of tumour growth as compared with inoculation of 143B cells transfected with control shRNA (Figure 6A). Kaplan–Meier analysis revealed that knockdown of *GLI2* in 143B cells provided a statistically significant survival benefit in mice (Figure 6B). These findings show that *GLI2* knockdown inhibits osteosarcoma cell growth in nude mice.

Discussion

Our findings demonstrate that GLI2 transcription factor significantly contributes to the growth of osteosarcoma cells. Our findings thus suggest that GLI2 might be an attractive target for therapeutic intervention, particularly in patients with high-grade and/or metastatic osteosarcoma. Small-molecule inhibitors of GLI transcription factors, such as GANT61, that efficiently inhibit the proliferation of prostate cancer cells have recently been identified [22]. MTT assay showed that GANT61 effectively inhibited osteosarcoma cell proliferation *in vitro*. We used 50 mg/kg GANT61 to inhibit GLI in a mouse xenograft model as previously described [22]. All injections were performed at a distance of 2–3 cm from the tumour site. We found no differences in osteosarcoma growth between the GANT61- and the control DMSO-treated groups (see Supporting information, Figure S1B). One possible explanation for this discrepancy is given by the difference in cell viability or permeation of GANT61

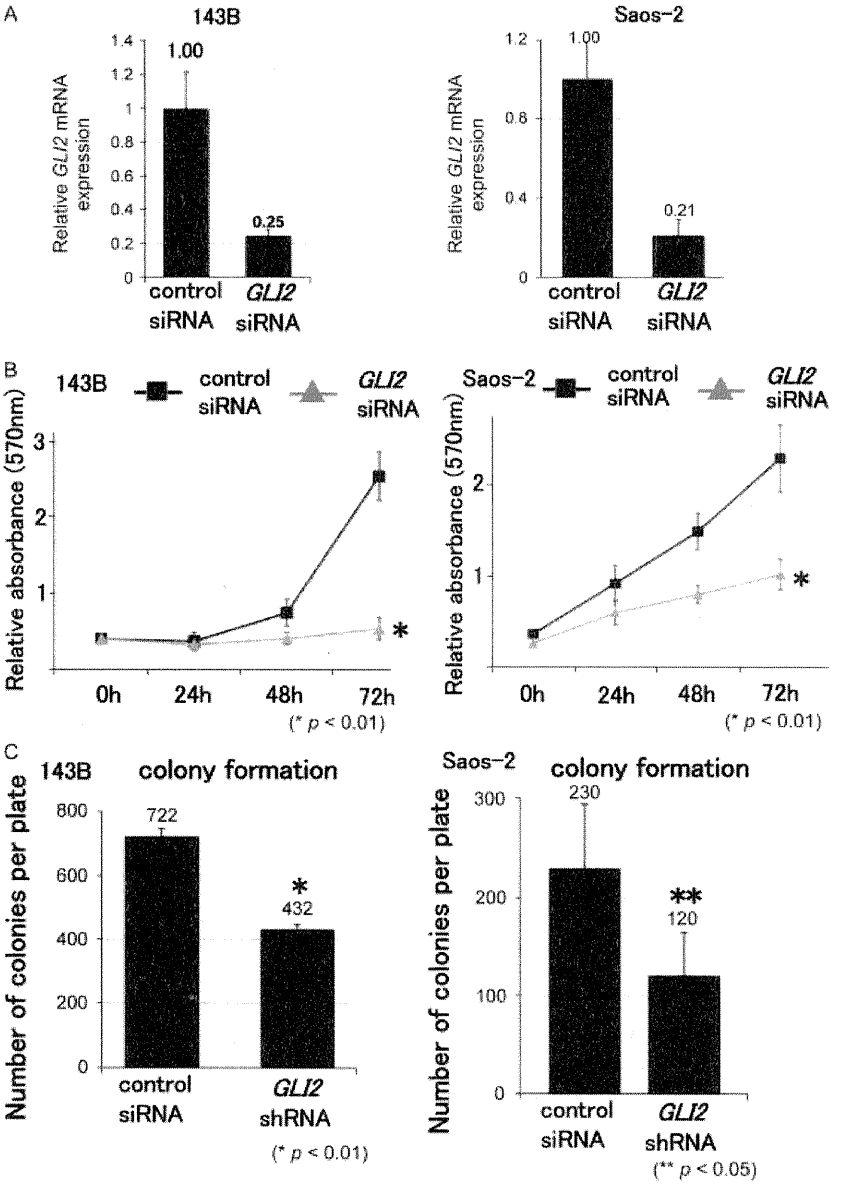

Figure 3. *GLI2* knockdown inhibits proliferation of osteosarcoma cells. (A) Transfection of *GLI2* siRNA resulted in a >70% knockdown efficiency of GLI2 [error bars represent mean (SD)]. $^{\Delta\Delta}$ Ct analysis was performed to evaluate the fold change in *GLI2* mRNA expression, using *GAPDH* or *ACTB*. (B) Growth at 72 h of 143B and Saos-2 cells was inhibited by *GLI2* siRNA. The experiment was performed in triplicate with similar results (*$p < 0.01$) [error bars represent mean (SD)]. (C) A reduced number of colonies was observed in soft agar following *GLI2* knockdown. These experiments were performed in triplicate with similar results (*$p < 0.01$; **$p < 0.05$) [error bars represent mean (SD)].

between the osteosarcoma and prostate cancer cells *in vivo*. Nonetheless, these two studies independently suggest that low-molecular-weight compounds can inhibit malignant tumours *in vitro*. Moreover, these findings suggest that other GLI-specific inhibitors may have a powerful therapeutic potential for the management of osteosarcoma and other malignancies characterized by constitutive activation of the Hedgehog signalling pathway.

For *in vivo GLI2* RNA interference studies, we inoculated 143B osteosarcoma cells that had been previously transfected with *GLI2* shRNA. Although knockdown of *GLI2* by shRNA significantly inhibited osteosarcoma growth in nude mice, this method is not clinically applicable. Recently, the potential clinical usefulness of RNA interference in mammalian cells has been demonstrated, with no reported interferon activation [25]. In addition, Davis *et al* [26] reported a human phase I clinical trial involving the systemic administration of siRNA to patients with solid cancers; they demonstrated that siRNA administered systemically to a human can inhibit a specific gene. These findings strongly suggest that administration of *GLI2* siRNA might be a promising new treatment for osteosarcoma.

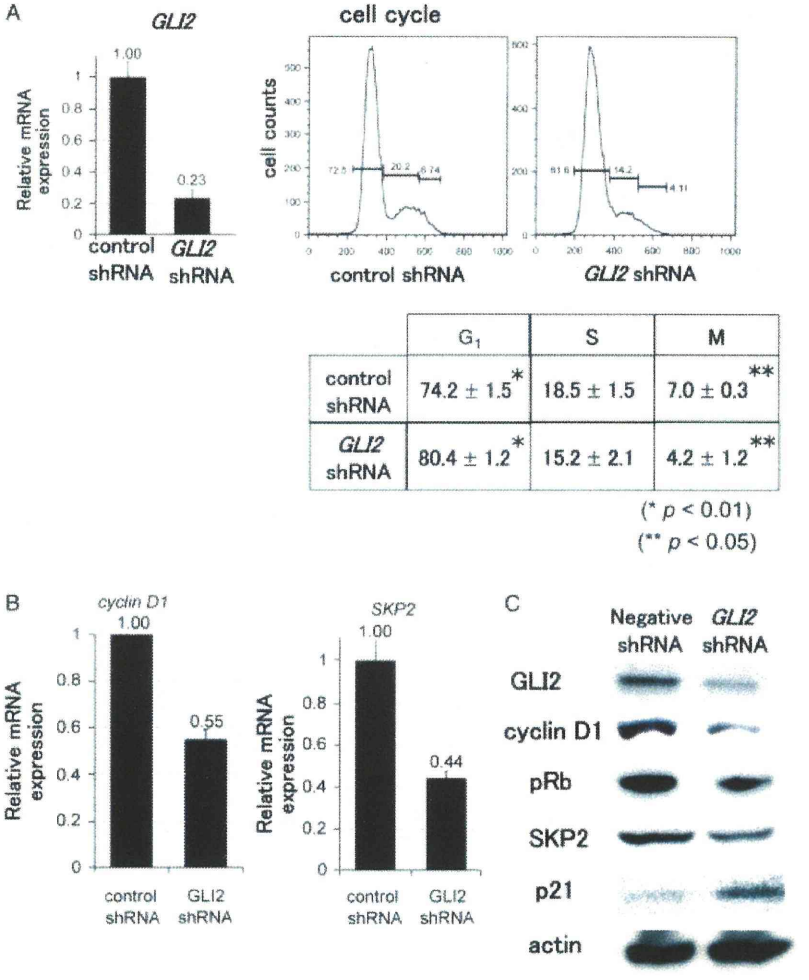

	G_1	S	M
control shRNA	74.2 ± 1.5*	18.5 ± 1.5	7.0 ± 0.3**
GLI2 shRNA	80.4 ± 1.2*	15.2 ± 2.1	4.2 ± 1.2**

(* $p < 0.01$)
(** $p < 0.05$)

Figure 4. Knockdown of *GLI2* promotes cell cycle arrest in the G_1 phase. (A) Following transfection of *GLI2* shRNA, the efficacy of *GLI2* knockdown was >75%. $^{\Delta\Delta}$ Ct analysis was performed to evaluate the fold change in mRNA expression, using *GAPDH* or *ACTB*. (B) When 143B cells were transfected with control shRNA, 74.2% of them were in G_1 phase, while when they were transfected with *GLI2* shRNA, 80.4% of the cells were in G_1 phase (*$p < 0.01$; **$p < 0.05$). (B) Real-time PCR was employed to examine the expression of cell cycle-related genes. $^{\Delta\Delta}$ Ct analysis was performed to evaluate fold changes of mRNA expression, using *GAPDH* or *ACTB*. Knockdown of *GLI2* decreased the expression of the cell cycle accelerators, *cyclin D1* and *SKP2* [error bars represent mean (SD)]. (C) Western blot analysis revealed that knockdown of *GLI2* decreased the protein levels of cyclin D1, pRb and SKP2. Western blot analysis revealed that knockdown of *GLI2* increased the expression of $p21^{cip1}$, a negative regulator of cell cycle progression.

We previously reported that inhibition of SMO by cyclopamine or by *SMO* RNA interference reduced the growth of osteosarcoma via cell cycle regulation [21]. Compared to several potential mutational targets within the Hedgehog pathway downstream of SMO already discovered, the group of tumours that would benefit from direct GLI inhibition is substantial and likely to increase. For instance, it has been reported that inhibition of GLI, but not SMO, induced apoptosis in chronic lymphocytic leukaemia cells [27].

In order to examine the molecular mechanisms of GLI2 up-regulation, we examine genomic amplification of the GLI2 locus. We performed cytogenetic studies in three osteosarcoma specimens. FISH analysis using specific probes for the GLI2 locus revealed no chromosomal abnormalities in our osteosarcoma biopsy tissues (data not shown); this region of the genome is known to be amplified in some tumour specimens [28–32]. Further examinations should be done to elucidate the molecular mechanisms of GLI2 up-regulation.

We showed that knockdown of *GLI2* decreased the expression of SKP2 [33,34]. In addition, we found that knockdown of *GLI2* increased the expression of $p21^{Cip1}$. SKP2 is a subunit of the SCF^{SKP2} complex, a ubiquitin-dependent ligase. Down-regulation of the SCF^{SKP2} complex may promote a cell cycle arrest in G_1 phase by inhibition of $p21^{Cip1}$ degradation. Several key signalling pathways, including Hedgehog, TGFβ, BMP, Notch and Wnt, are engaged in essential processes of embryonic development. Recently, it has been clarified that these pathways also play important roles in the pathogenesis of malignant tumours (reviewed in [35]). In addition, it has been shown that there is a direct interaction or crosstalk among these key pathways (reviewed in [36]). We previously reported that

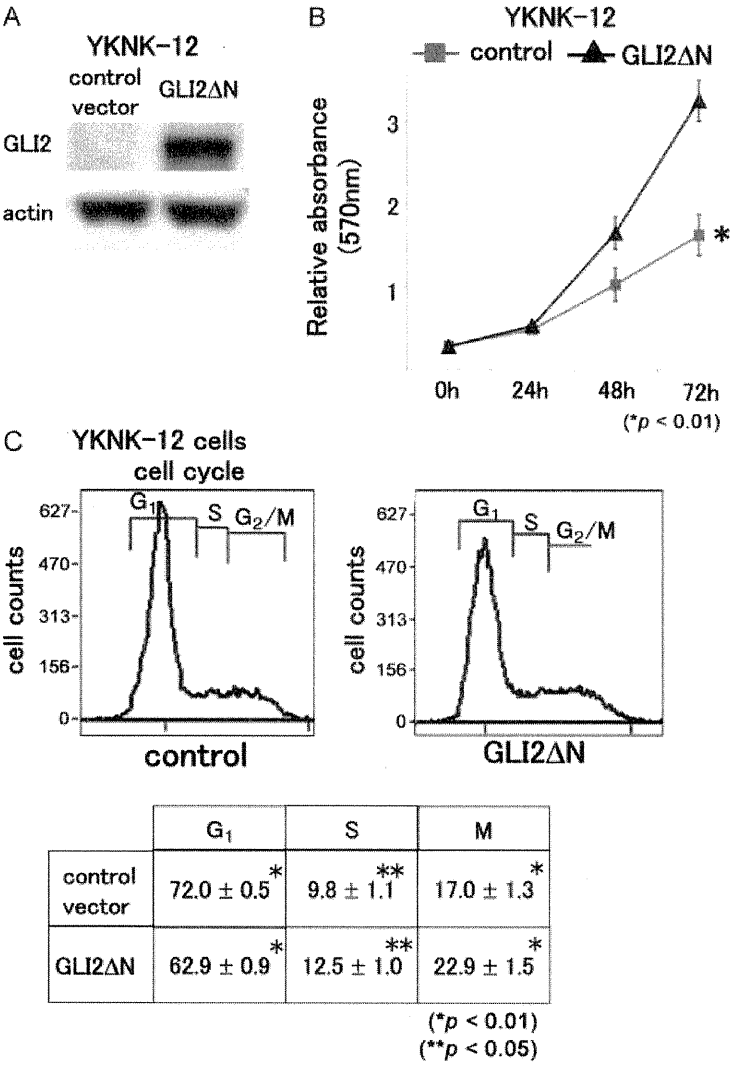

	G_1	S	M
control vector	72.0 ± 0.5*	9.8 ± 1.1**	17.0 ± 1.3*
GLI2ΔN	62.9 ± 0.9*	12.5 ± 1.0**	22.9 ± 1.5*

(*$p < 0.01$)
(**$p < 0.05$)

Figure 5. Over-expression of GLI2 accelerates mesenchymal stem cell proliferation. (A) Western blot analysis revealed that cells transfected with the GLI2ΔN expression vector reacted positively with the anti-GLI2 antibody. (B) We assessed the proliferation of YKNK-12 cells following transfection with the GLI2ΔN expression vector, which exhibits a potent transcriptional activity. The MTT assay showed that forced expression of GLI2ΔN promoted YKNK-12 cell proliferation to a greater extent than transfection with control vector (*$p < 0.01$) [error bars represent mean (SD)]. (C) Cell cycle analysis of YKNK-12 cell revealed that 62.9% and 72.0% of the cells were in G_1 phase following forced expression of GLI2ΔN and transfection with control vector, respectively. Furthermore following forced expression of GLI2ΔN, 12.5% and 22.9% of the cells were in the S and G_2–M phase, respectively, whereas 9.8% and 17.0% of the control vector-transfected cells were in the S and G_2–M phase, respectively (*$p < 0.01$; **$p < 0.05$).

the Notch pathway is activated in human osteosarcoma and that its activation promotes osteosarcoma cell growth [37]. In turn, activation of the Notch pathway promotes transcription of SKP2. SKP2 might thus mediate the crosstalk between the Notch and Hedgehog pathways. Further studies are needed to elucidate the role of interaction between these pathways in the pathogenesis of osteosarcoma.

Several recent studies have demonstrated that the anti-tumour effects of Hedgehog pathway inhibitors are mediated by their effects on tumour stromal cells [38,39]. Other studies have demonstrated that Hedgehog pathway inhibitors directly affect cancer cells [21,22,40–44]. Our findings showed that both GLI inhibition and *GLI2* knockdown directly inhibit osteosarcoma cell growth. Further studies are needed to establish the role of GLI2 activation in response to paracrine and autocrine Hedgehog signalling in osteosarcoma cells.

The hypothesis that malignant tumours are generated by rare populations of tumour-initiating cells (TICs), also called cancer stem cells, that are more tumourigenic than other cancer cells, has gained increasing credence [22,45]. We and others have reported that some bone and soft tissue sarcomas are generated by TICs [16,46]. The Hedgehog pathway has been implicated in the maintenance of normal stem cell or progenitor cells in many tissues, including the epithelia of many internal organs and brain [47]. Magali *et al* [48,49] reported that inhibition of Hedgehog

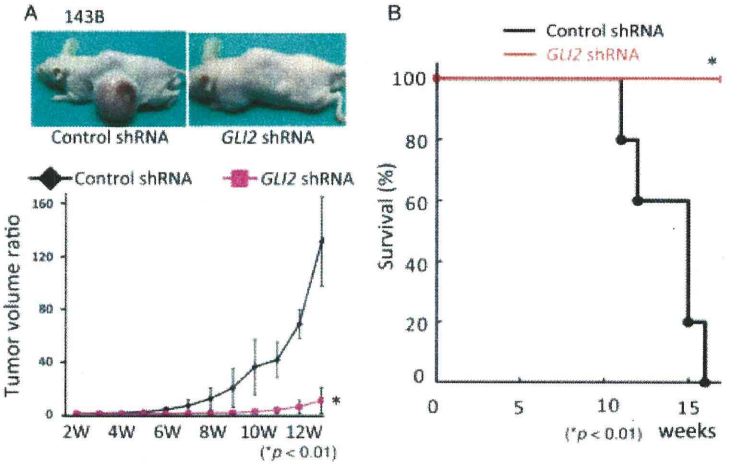

Figure 6. *GLI2* knockdown inhibits osteosarcoma growth in nude mice. (A) Following transfection of control shRNA or *GLI2* shRNA, 1×10^6 143 B cells were subcutaneously inoculated in nude mice. Tumour size was calculated weekly by using the formula $LW^2/2$ (where L and W represent the length and width of tumours). Seven days after inoculation, tumour volume was set as 1 and the increase in tumour volume was calculated at different time points, using the above formula. *GLI2* shRNA-transfected cells demonstrated a significant inhibition of tumour growth as compared with control shRNA-transfected cells ($n = 6$; $^*p < 0.01$) [error bars represent mean (SD)]. Kaplan–Meier analysis revealed that knockdown of *GLI2* provided a significant survival benefit ($n = 6$; $^*p < 0.01$).

signalling depletes TICs, whereas constitutive activation of Hedgehog signalling increases the number of TICs and accelerates tumour progression. These findings suggest that inhibition of the Hedgehog pathway might decrease the proportion of osteosarcoma TICs. The presence of a high aldehyde dehydrogenase (ALDH) activity has been used to identify TICs in malignant tumours [50–52]. Recently, Wang *et al* [53] reported that TICs obtained from osteosarcoma can be identified by a high ALDH activity. In this regard, we determined the proportion of cells with a high ALDH activity following *GLI2* siRNA transfection. At baseline, 30.6% of 143B cells showed a high ALDH activity. Seven days after *GLI2* siRNA transfection, there was no change in the proportion of cells with a high ALDH activity (data not shown). Further studies are needed to determine the impact of Hedgehog pathway inhibition on the proportion of TICs in other osteosarcoma cell lines or using other methodologies to identify TICs. In conclusion, our findings demonstrate that inhibition of GLI2 prevents osteosarcoma growth. These finding improves our understanding of osteosarcoma pathogenesis and suggest that inhibitions of GLI2 may be regarded as an effective treatment for patients with osteosarcoma.

Acknowledgment

We are grateful to Hui Gao for excellent technical assistance. We thank Dr Naoya Kobayashi (Department of Surgery, Okayama University Graduate School of Medicine and Dentistry, Japan) for providing the YKNK-12 cell line. We thank H Sasaki (Laboratory for Embryonic Induction, RIKEN Centre for Developmental Biology, Kobe, Japan) for providing the reporter vectors. This work was supported by Grants-in-Aid for Scientific Research (KAKENHI) (B) 18390419, (C) 19591725, (C) 20591786, (C) 21591919, (C) 21591920, and (C) 22591663 and a Grant-in-Aid from the Ministry of Health, Labour, and Welfare of Japan for the Third Term Comprehensive Control Research for Cancer.

Author contributions

NH, IY, NS, KS and ST conceived and designed the experiments. NH, HM, YT and TT performed the experiments. IK, NK, KS and ST analysed the data. NH and HM contributed reagents/materials/analysis tools. ST drafted the manuscript.

References

1. Sweetnam R. Osteosarcoma. *Br J Hosp Med* 1982; **28**: .116 112–121.
2. Dorfman HD, Czerniak B. Bone cancers. *Cancer* 1995; **75**: 203–210.
3. Wu PK, Chen WM, Chen CF, *et al*. Primary osteogenic sarcoma with pulmonary metastasis: clinical results and prognostic factors in 91 patients. *Japan J Clin Oncol* 2009; **39**: 514–522.
4. Iwamoto Y, Tanaka K, Isu K, *et al*. Multi-institutional phase II study of neoadjuvant chemotherapy for osteosarcoma (NECO study) in Japan: NECO-93J and NECO-95J. *J Orthop Sci* 2009; **14**: 397–404.
5. Meyers PA, Schwartz CL, Krailo M, *et al*. Osteosarcoma: a randomized, prospective trial of the addition of ifosfamide and/or muramyl tripeptide to cisplatin, doxorubicin, and high-dose methotrexate. *J Clin Oncol* 2005; **23**: 2004–2011.
6. Kager L, Zoubek A, Kastner U, *et al*. Skip metastases in osteosarcoma: experience of the Cooperative Osteosarcoma Study Group. *J Clin Oncol* 2006; **24**: 1535–1541.
7. Horowitz JM, Park SH, Bogenmann E, *et al*. Frequent inactivation of the retinoblastoma anti-oncogene is restricted to a subset of human tumor cells. *Proc Natl Acad Sci USA* 1990; **87**: 2775–2779.

8. Ingham PW, McMahon AP. Hedgehog signaling in animal development: paradigms and principles. *Genes Dev* 2001; **15**: 3059–3087.
9. Ruiz i Altaba A, Sanchez P, Dahmane N. Gli and hedgehog in cancer: tumours, embryos and stem cells. *Nat Rev* 2002; **2**: 361–372.
10. Lum L, Beachy PA. The Hedgehog response network: sensors, switches, and routers. *Science (NY)* 2004; **304**: 1755–1759.
11. Bijlsma MF, Spek CA, Peppelenbosch MP. Hedgehog: an unusual signal transducer. *Bioessays* 2004; **26**: 387–394.
12. Ding Q, Motoyama J, Gasca S, *et al*. Diminished sonic hedgehog signaling and lack of floor plate differentiation in *Gli2* mutant mice. *Development (Camb UK)* 1998; **125**: 2533–2543.
13. Ruiz i Altaba A, Mas C, Stecca B. The *Gli* code: an information nexus regulating cell fate, stemness and cancer. *Trends Cell Biol* 2007; **17**: 438–447.
14. Nakahara H, Misawa H, Hayashi T, *et al*. Bone repair by transplantation of hTERT-immortalized human mesenchymal stem cells in mice. *Transplantation* 2009; **88**: 346–353.
15. Hijioka H, Setoguchi T, Miyawaki A, *et al*. Up-regulation of Notch pathway molecules in oral squamous cell carcinoma. *Int J Oncol* 2010; **36**: 817–822.
16. Hirotsu M, Setoguchi T, Matsunoshita Y, *et al*. Tumour formation by single fibroblast growth factor receptor 3-positive rhabdomyosarcoma-initiating cells. *Br J Cancer* 2009; **101**: 2030–2037.
17. Sasaki H, Hui C, Nakafuku M, *et al*. A binding site for Gli proteins is essential for HNF-3β floor plate enhancer activity in transgenics and can respond to Shh *in vitro*. *Development (Camb, UK)* 1997; **124**: 1313–1322.
18. Sasaki H, Nishizaki Y, Hui C, *et al*. Regulation of Gli2 and Gli3 activities by an amino-terminal repression domain: implication of Gli2 and Gli3 as primary mediators of Shh signaling. *Development (Camb, UK)* 1999; **126**: 3915–3924.
19. Fukushima M, Setoguchi T, Komiya S, *et al*. Retinal astrocyte differentiation mediated by leukemia inhibitory factor in cooperation with bone morphogenetic protein 2. *Int J Dev Neurosci* 2009; **27**: 685–690.
20. Sasaki H, Setoguchi T, Matsunoshita Y, *et al*. The knock-down of over-expressed EZH2 and BMI-1 does not prevent osteosarcoma growth. *Oncology Rep* 2010; **23**: 677–684.
21. Hirotsu M, Setoguchi T, Sasaki H, *et al*. Smoothened as a new therapeutic target for human osteosarcoma. *Mol Cancer* 2010; **9**: 5.
22. Lauth M, Bergstrom A, Shimokawa T, *et al*. Inhibition of GLI-mediated transcription and tumor cell growth by small-molecule antagonists. *Proc Natl Acad Sci USA* 2007; **104**: 8455–8460.
23. Tang N, Song WX, Luo J, *et al*. Osteosarcoma development and stem cell differentiation. *Clin Orthop Rel Res* 2008; **466**: 2114–2130.
24. Roessler E, Ermilov AN, Grange DK, *et al*. A previously unidentified amino-terminal domain regulates transcriptional activity of wild-type and disease-associated human *GLI2*. *Hum Mol Genet* 2005; **14**: 2181–2188.
25. Elbashir SM, Harborth J, Lendeckel W, *et al*. Duplexes of 21-nucleotide RNAs mediate RNA interference in cultured mammalian cells. *Nature* 2001; **411**: 494–498.
26. Davis ME, Zuckerman JE, Choi CH, *et al*. Evidence of RNAi in humans from systemically administered siRNA via targeted nanoparticles. *Nature* 2010; **464**: 1067–1070.
27. Desch P, Asslaber D, Kern D, *et al*. Inhibition of GLI, but not Smoothened, induces apoptosis in chronic lymphocytic leukemia cells. *Oncogene* 2010; **29**: 4885–4895.
28. Gimenez S, Costa C, Espinet B, *et al*. Comparative genomic hybridization analysis of cutaneous large B-cell lymphomas. *Exp Dermatol* 2005; **14**: 883–890.
29. Fishman A, Shalom-Paz E, Fejgin M, *et al*. Comparing the genetic changes detected in the primary and secondary tumor sites of ovarian cancer using comparative genomic hybridization. *Int J Gynecol Cancer* 2005; **15**: 261–266.
30. Liu XP, Sato T, Oga A, *et al*. Two subtypes of mucinous colorectal carcinoma characterized by laser scanning cytometry and comparative genomic hybridization. *Int J Oncol* 2004; **25**: 615–621.
31. Wreesmann VB, Ghossein RA, Hezel M, *et al*. Follicular variant of papillary thyroid carcinoma: genome-wide appraisal of a controversial entity. *Genes Chromosomes Cancer* 2004; **40**: 355–364.
32. Wei G, Lonardo F, Ueda T, *et al*. *CDK4* gene amplification in osteosarcoma: reciprocal relationship with *INK4A* gene alterations and mapping of 12q13 amplicons. *Int J Cancer* 1999; **80**: 199–204.
33. Kamura T, Hara T, Matsumoto M, *et al*. Cytoplasmic ubiquitin ligase KPC regulates proteolysis of p27(Kip1) at G_1 phase. *Nat Cell Biol* 2004; **6**: 1229–1235.
34. Hara T, Kamura T, Kotoshiba S, *et al*. Role of the UBL-UBA protein KPC2 in degradation of p27 at G_1 phase of the cell cycle. *Mol Cell Biol* 2005; **25**: 9292–9303.
35. Rubin LL, de Sauvage FJ. Targeting the Hedgehog pathway in cancer. *Nat Rev Drug Discov* 2006; **5**: 1026–1033.
36. Ross J, Li L. Recent advances in understanding extrinsic control of hematopoietic stem cell fate. *Curr Opin Hematol* 2006; **13**: 237–242.
37. Tanaka M, Setoguchi T, Hirotsu M, *et al*. Inhibition of Notch pathway prevents osteosarcoma growth by cell cycle regulation. *Br J Cancer* 2009; **100**: 1957–1965.
38. Tian H, Callahan CA, DuPree KJ, *et al*. Hedgehog signaling is restricted to the stromal compartment during pancreatic carcinogenesis. *Proc Natl Acad Sci USA* 2009; **106**: 4254–4259.
39. Yauch RL, Gould SE, Scales SJ, *et al*. A paracrine requirement for hedgehog signalling in cancer. *Nature* 2008; **455**: 406–410.
40. Sanchez P, Hernandez AM, Stecca B, *et al*. Inhibition of prostate cancer proliferation by interference with sonic hedgehog–GLI1 signaling. *Proc Natl Acad Sci USA* 2004; **101**: 12561–12566.
41. Singh RR, Cho-Vega JH, Davuluri Y, *et al*. Sonic hedgehog signaling pathway is activated in ALK-positive anaplastic large cell lymphoma. *Cancer Res* 2009; **69**: 2550–2558.
42. Lindemann RK. Stroma-initiated hedgehog signaling takes center stage in B-cell lymphoma. *Cancer Res* 2008; **68**: 961–964.
43. Wong SY, Seol AD, So PL, *et al*. Primary cilia can both mediate and suppress Hedgehog pathway-dependent tumorigenesis. *Nat Med* 2009; **15**: 1055–1061.
44. Dierks C, Beigi R, Guo GR, *et al*. Expansion of *Bcr-Abl*-positive leukemic stem cells is dependent on Hedgehog pathway activation. *Cancer Cell* 2008; **14**: 238–249.
45. Clarke MF, Fuller M. Stem cells and cancer: two faces of Eve. *Cell* 2006; **124**: 1111–1115.
46. Murase M, Kano M, Tsukahara T, *et al*. Side population cells have the characteristics of cancer stem-like cells/cancer-initiating cells in bone sarcomas. *Br J Cancer* 2009; **101**: 1425–1432.
47. Beachy PA, Karhadkar SS, Berman DM. Tissue repair and stem cell renewal in carcinogenesis. *Nature* 2004; **432**: 324–331.
48. Dierks C, Grbic J, Zirlik K, *et al*. Essential role of stromally induced hedgehog signaling in B-cell malignancies. *Nat Med* 2007; **13**: 944–951.
49. Zhao C, Chen A, Jamieson CH, *et al*. Hedgehog signalling is essential for maintenance of cancer stem cells in myeloid leukaemia. *Nature* 2009; **458**: 776–779.
50. Ginestier C, Hur MH, Charafe-Jauffret E, *et al*. ALDH1 is a marker of normal and malignant human mammary stem cells and a predictor of poor clinical outcome. *Cell Stem Cell* 2007; **1**: 555–567.

51. Huang EH, Hynes MJ, Zhang T, *et al*. Aldehyde dehydrogenase 1 is a marker for normal and malignant human colonic stem cells (SC) and tracks SC overpopulation during colon tumorigenesis. *Cancer Res* 2009; **69**: 3382–3389.
52. Cheung AM, Wan TS, Leung JC, *et al*. Aldehyde dehydrogenase activity in leukemic blasts defines a subgroup of acute myeloid leukemia with adverse prognosis and superior NOD/SCID engrafting potential. *Leukemia* 2007; **21**: 1423–1430.
53. Wang L, Park P, Zhang H, *et al*. Prospective identification of tumorigenic osteosarcoma cancer stem cells in OS99–1 cells based on high aldehyde dehydrogenase activity. *Int J Cancer* 2011; **128**: 294–303.

SUPPORTING INFORMATION ON THE INTERNET

The following supporting information may be found in the online version of this article:

Figure S1. Knockdown of GLI2 promotes cell arrest of Saos-2 cell.

Incidence of Outer Foveal Defect After Macular Hole Surgery

HIROKI KAWANO, AKINORI UEMURA, AND TAIJI SAKAMOTO

• PURPOSE: **To determine the incidence of outer foveal defects after macular hole surgery and to evaluate the relationship between the defect and visual outcome.**
• DESIGN: **Retrospective, observational case series.**
• METHODS: **A retrospective analysis was performed on 50 eyes from 50 patients who underwent macular hole surgery with a follow-up period of 12 months or more. We evaluated the presence of outer foveal defects using time-domain optical coherence tomography and best-corrected visual acuity at several postoperative time points. The main outcome measures are the incidence of an outer foveal defect and the best-corrected visual acuity.**
• RESULTS: **The incidence of an outer foveal defect at 1, 3, 6, and 12 months after surgery was 49%, 50%, 47%, and 31%, respectively. There were no statistical differences in the postoperative visual acuity between eyes with and without an outer foveal defect at each postoperative time point.**
• CONCLUSIONS: **Outer foveal defects after successful macular hole surgery were observed in approximately half of the eyes during the early postoperative period and one third of the eyes at 12 months postoperatively, suggesting that it takes longer than expected to recover the normal foveal anatomy after surgery. The presence of outer foveal defects did not significantly correlate with the visual outcome.** **(Am J Ophthalmol 2011;151:318–322.** © **2011 by Elsevier Inc. All rights reserved.)**

SINCE THE INTRODUCTION OF VITRECTOMY FOR THE treatment of macular hole in 1991, vitreous surgery has become the standard in therapy for the disease.[1] The success rate of macular hole surgery after the introduction of the internal limiting membrane peeling technique has been reported to be as high as 85% to 100%.[2–4]

Optical coherence tomography (OCT) has become the gold standard for the diagnosis of macular hole and for confirming the anatomic closure of the macular hole after surgery. Recent innovations in OCT enable the detailed observation of retinal anatomy, including the photoreceptor layer. Previous reports suggested that repair of the photoreceptor layer was associated with visual improvement after macular hole surgery.[5–11]

In the process of macular hole closure, bridging of the inner retina was first observed.[12] In the early postoperative period, therefore, OCT occasionally demonstrated hyporeflective defects in the outer fovea.[13–15] In fact, several reports have documented the hyporeflective defects using OCT after macular hole surgery or after spontaneous closure of macular holes.[9–11,16] However, there is little information about the incidence of this anatomic change following macular hole surgery.[7,9] Additionally, the relationship between the presence of outer foveal defects and the visual outcome has not been fully understood.

The purpose of this study was to determine the incidence of an outer foveal defect after successful macular hole surgery. Also, we investigated the possible correlation between the presence of an outer foveal defect and the visual outcome.

METHODS

WE RETROSPECTIVELY REVIEWED PATIENT RECORDS TO identify patients who underwent pars plana vitrectomy for idiopathic macular holes performed by a single surgeon between December 1, 2004 and July 31, 2008 at a single, referral-based hospital. Inclusion criteria were stage 2-4 idiopathic macular hole and a 12-month or longer follow-up after surgery. Patients with myopia greater than 6 diopters, symptoms longer than 12 months, or history of vitreous surgery were excluded. Also excluded from the study were patients with failure to close the macular hole. Therefore, a total of 50 eyes from 50 patients (15 male and 35 female; mean age, 65.6 years) were included in this study. The study included 19 in stage 2 macular hole, 22 in stage 3, and 9 in stage 4. The staging of the macular hole was determined by slit-lamp examination and classified according to Gass classification.

Surgery was performed by a single surgeon. Informed consent was obtained prior to surgical intervention in all patients. A standard 3-port pars plana vitrectomy was performed in all patients using retrobulbar anesthesia. The crystalline lens was removed by phacoemulsification followed by intraocular lens implantation before pars plana vitrectomy in phakic eyes. After core vitrectomy, the posterior vitreous was separated from the retina, if still

Accepted for publication Aug 18, 2010.
From the Department of Ophthalmology, Kagoshima City Hospital, Kagoshima, Japan (H.K., A.U.); and the Department of Ophthalmology, Kagoshima University Graduate School of Medicine and Dental Sciences, Kagoshima, Japan (H.K., T.S.).
Inquiries to Akinori Uemura, Department of Ophthalmology, Kagoshima City Hospital, 20-17 Kajiya-cho, Kagoshima-shi, Kagoshima 892-8580, Japan; e-mail: akiu@ml.kch.kagoshima.kagoshima.jp

0002-9394/$36.00
doi:10.1016/j.ajo.2010.08.034

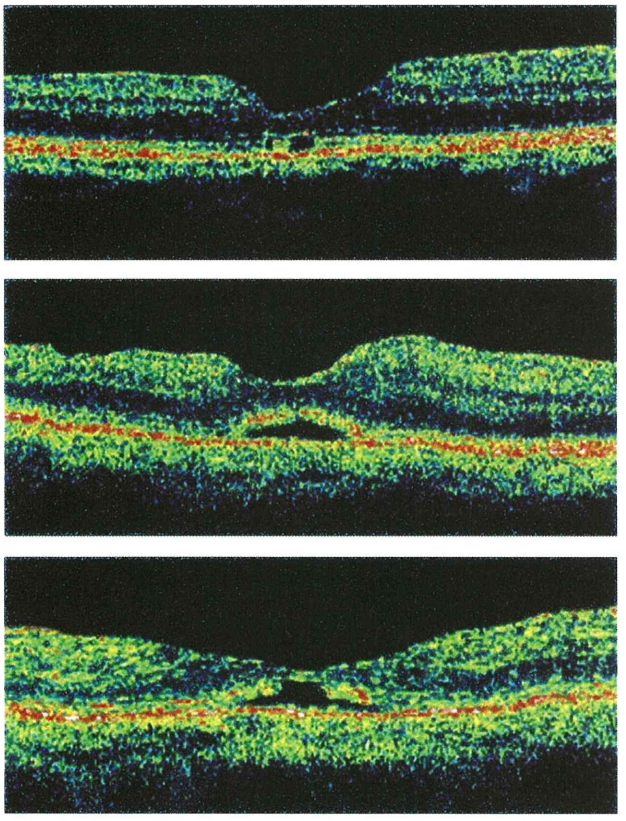

FIGURE 1. Tomographic features of an outer foveal defect after macular hole surgery. Outer layer defect with (Top) a disruption of an inner and outer segment (IS/OS) line, (Middle) a foveal detachment with a continuous IS/OS line, and (Bottom) a foveal detachment with a disruption of IS/OS line.

attached. The internal limiting membrane (ILM) peeling was performed using a microvitreoretinal blade and vitreoretinal forceps after staining the ILM with triamcinolone acetonide. After a fluid-air exchange, an air-gas exchange was performed using 20% sulfur hexafluoride (SF6), and the patient was asked to maintain a face-down position for at least 5 days.

The patients underwent complete ophthalmologic examinations including best-corrected visual acuity measurements, slit-lamp biomicroscopy, indirect ophthalmoscopy, fundus photography, and OCT examinations. Before surgery, the macular hole size was recorded using OCT, specifying its minimum, or aperture, diameter from the closest lip of the hole to its center. Preoperative examinations were performed the day before the macular hole surgery, and follow-up was scheduled at 1, 3, 6, and 12 months after the surgery. At each visit, all patients underwent visual acuity measurements, indirect ophthalmoscopy, slit-lamp examinations, fundus photographs, and OCT.

OCT examinations were performed using Stratus OCT (Carl Zeiss Meditec, Inc, Humphrey Division, Dublin, California, USA) after pupil dilation using fixation on an internal target to define the center of the fovea and recording 10 horizontal transfoveal scans and 10 vertical scans by a single expert examiner. Particular attention was paid to the outer layers of the fovea, especially outer foveal hyporeflective defects over the retinal pigment epithelium (RPE). If at least 1 of the scans showed an outer foveal defect, the scans from that eye were selected for analysis.

The definition of outer foveal defect for the purpose of this study was the appearance of an outer foveal hyporeflective defect on OCT images. We divided the outer foveal defects seen on OCT into 4 groups: outer layer defect, foveal detachment, complex, and unclassified (Figure 1). The outer layer defect type included a complete disruption of the photoreceptor inner and outer segment (IS/OS) junction with a hyporeflective empty space between them. The foveal detachment type included an elevation of the outer foveal layer with a continuous IS/OS junction. The complex type demonstrated foveal detachment with a disruption of IS/OS junction.

Visual acuity data were converted to the logarithm of the minimal angle of resolution (logMAR) and analyzed using StatView software (Abacus; Abacus Concepts, Inc., Berkeley, California, USA). The *t* test was used to compare preoperative and postoperative visual acuities.

RESULTS

THE INCIDENCE OF AN OUTER FOVEAL DEFECT AT 1, 3, 6, and 12 months was 49% (23/47), 50% (21/42), 47% (17/36), and 31% (15/48), respectively (Table 1). The types of outer foveal defects in the 23 eyes at 1 month included outer layer defects in 18 eyes (78%) and foveal detachment in 4 eyes (17%). At 12 months, all 15 eyes with defects were classified as outer foveal layer defects (Figure 2).

We compared the preoperative and postoperative characteristics between eyes with and without an outer foveal defect at each visit. There were no statistical differences in visual acuity at the 12-month follow-up time point between eyes with and without defects (Table 2). Also, preoperative macular hole stage was not associated with the presence of defects. Eyes without an outer foveal defect had better improvement in visual acuity, but the difference was not statistically significant. Similar results were found at the 1-, 3-, and 6-month follow-up examinations, although preoperative macular hole size was significantly smaller in eyes with a defect than in eyes without a defect at the 1-month visit (365 μm vs 464 μm).

TABLE 1. Type of Outer Foveal Defect at Each Postoperative Period

	Postoperative Time			
	1 Month	3 Months	6 Months	12 Months
Outer layer defect	18 (78%)	20 (95%)	16 (94%)	15 (100%)
Foveal detachment	4 (17%)	1 (5%)	0	0
Combined	1 (4%)	0	0	0
Unclassified	0	0	1 (6%)	0
Total	23/47 (49%)	21/42 (50%)	17/36 (47%)	15/48 (31%)

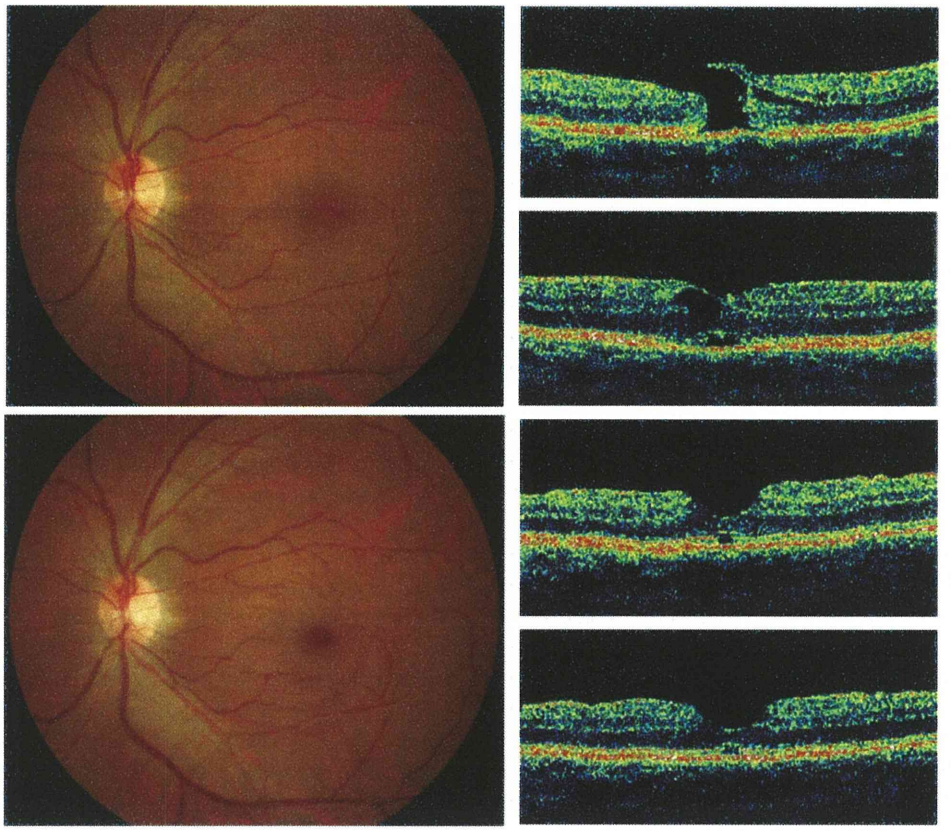

FIGURE 2. A persistent outer foveal defect after macular hole surgery in a 62-year-old man. (Top left) Preoperative fundus photograph showing a macular hole in the left eye. (Bottom left) Fundus photograph at 12 months postoperatively showing a closed macular hole. (Top right) Preoperative optical coherence tomography (OCT) shows a stage 2 macular hole. The visual acuity is 20/100. (Second row right) Postoperative (1-month) OCT image shows a closed macular hole with an outer foveal defect. Visual acuity is 20/50. (Third row right) Postoperative (6-month) OCT image demonstrates a persistent outer foveal defect. Visual acuity is 20/20. (Bottom right) Postoperative (12-month) OCT image still demonstrates a defect of the outer fovea. Visual acuity is 20/20.

DISCUSSION

THE PRESENCE OF A SUBFOVEAL HYPOREFLECTIVE SPACE on OCT image after macular hole surgery has been observed since the introduction of the first-generation OCT. Takahashi and Kishi reported on a series of 25 eyes with successfully closed macular holes, 44% of which had a bridge formation of the tissue continuous with the inner retina within 1 month after surgery.[12] Recent innovations in OCT technology have revealed the detailed foveal anatomy, including the photoreceptor layer, leading to a more detailed analysis of macular pathology after surgery. Several reports have described the importance of the foveal photoreceptor layer and the relationship between the disruption of the photoreceptor layer and visual outcomes.[5–11] Therefore, the presence of an outer foveal

TABLE 2. Comparison of Clinical Features Between Eyes With and Without Outer Foveal Defects at 12-Month Follow-up

	Outer Foveal Defect		
	Present	Absent	*P* Value
Number of eyes	15	33	
Female gender	66%	70%	.54
Mean age, years	67.7	64.5	.21
Preoperative MH diameter, μm	419.3	407.1	.80
Preoperative VA logMAR (decimal)	0.69 (0.20)	0.84 (0.14)	.09
Postoperative VA logMAR (decimal)	0.13 (0.75)	0.13 (0.74)	.92
Improvement of VA logMAR (Preoperative-12 months)	0.56	0.71	.08

logMAR = logarithm of minimal angle of resolution; MH = macular hole; VA = visual acuity.

defect was thought to interfere with postoperative visual improvement.[13] However, little is known about the incidence of defects in the macular hole surgery postoperative course and the relationship between defects and visual outcomes.

In the current study, outer foveal defects after uneventful macular hole surgery were observed in half of the patients at the early postoperative periods. Interestingly, only one third of the patients still had the defect at 12 months after surgery. Previous reports have described the incidence of hyporeflective defects after macular hole surgery. Sano and associates observed foveal detachments in 43% of eyes at 1 month and in 25% at 6 months after macular hole surgery using spectral-domain OCT.[9] In their report, there was no obvious description of the difference between a foveal detachment and an outer foveal defect. Ko and associates reported the incidence of an outer foveal defect after macular hole surgery using ultrahigh-resolution OCT: outer foveal defects were observed in 65% of the eyes and persistent foveal detachments in 18%.[14] Because the patients underwent OCT examination at various postoperative intervals, we cannot compare the results with those of our study. Baba and associates observed subretinal gaps in 17% of eyes 6 months after macular hole surgery using Stratus OCT.[7] Christensen and colleagues found persistent subfoveal fluid in one third of eyes at 3 months after macular hole surgery and in 6.8% at 12 months after surgery.[17]

The incidence of an outer foveal defect in the current study was higher than those in previous reports, despite the use of time-domain OCT. Although the real reason for the high incidence is unknown, we speculate that detailed OCT examinations searching for abnormalities of the outer fovea may have resulted in the high incidence rate of the defect. Therefore, it is expected that the incidence would have been even higher in the prospective study using a high-resolution OCT. In fact, Inoue and associates reported a detailed analysis of the photoreceptor layer after macular hole surgery using spectral-domain OCT, and observed IS/OS junction abnormalities in 93% of patients at the 12-month follow-up.[11] These observations suggest that outer foveal defects were present at a higher rate than expected not only at the early postoperative time point but also at 12 months after surgery.

We defined outer foveal defect as a hyporeflective empty space directly below the center of the fovea in this series. Most outer foveal defects were divided into 3 patterns: a disrupted IS/OS line, a foveal detachment with continuous IS/OS line, and a foveal detachment with a disrupted IS/OS line. Although foveal detachments were seen in 21% of eyes at the early postoperative period, all outer foveal defects at the 12-month follow-up were IS/OS disruption type. Although these empty spaces are thought to be the result of bridging of the inner retinal layers in the early postoperative period, the current study could not demonstrate how the empty space was formed.

There have been no reports concerning the preoperative clinical factors associated with the development of an outer foveal defect. In our study, there were no significant factors associated with the presence of outer foveal defects that were observed at 12-month follow-up. The only relevant factor was the preoperative macular hole size, which was related to the defect observed at 1 month postoperatively, but not at the 3-, 6-, and 12-month follow-ups. It is probable, in a small macular hole, that a bridge formation is likely to develop in the early postoperative period before the reapproximation of the outer fovea.

Several reports have documented the relationship between the presence of an outer foveal defect and postoperative visual acuity. In this series, we found that the presence of an outer foveal defect was not associated with visual outcome at each time point. Sano and associates showed that visual acuity was significantly better in eyes with a continuous IS/OS line compared to eyes with a disrupted IS/OS line, in spite of the presence or absence of outer foveal defects.[9] These facts might indicate that visual acuity is determined not by the presence or absence of defects but by the disruption of the photoreceptor layer. Previous reports have documented that larger disruption of the photoreceptor layer was associated with a poorer visual acuity after macular hole surgery.[5–11] Therefore, despite the presence of an outer foveal defect below the center of the fovea, favorable visual acuity outcomes may be possible when the defect is small and the photoreceptor layer around the defect is relatively normal on an OCT image.[15]

This study has several limitations. The most important limitation of the present study is that it is not a prospective investigation. Additionally, we used a time-domain OCT

in this study. Therefore, the percentage of eyes with an outer foveal defect may have been underestimated in our retrospective series. However, these limitations do not change the fact that the presence of an outer foveal defect on OCT is higher than expected even in the long-term follow-up measurements.

In conclusion, an outer foveal defect after successful macular hole surgery was observed in half of the eyes at the early postoperative time point and in one third at 12 months postoperatively. After macular surgery, anatomic recovery of the fovea might be gradual and take more than a year to reach its maximum, as shown in the functional recovery. The visual outcome may not be dependent on the presence or absence of an outer foveal defect, but rather on the size of the defect or the status of the photoreceptor layer around the defect. Therefore, macular hole surgeons should know that the presence of a defect after macular hole surgery is common and not a source of grave concern. Further studies with longer follow-up times using high-resolution OCT are needed to understand the pathogenesis of outer foveal defects.

THE AUTHORS INDICATE NO FINANCIAL SUPPORT OR FINANCIAL CONFLICT OF INTEREST. INVOLVED IN DESIGN OF THE study (A.U.); conduct of the study (A.U.); collection of data (H.K., A.U.); management, analysis, and interpretation of data (A.U., T.S.); and preparation, review, and approval of manuscript (H.K., A.U., T.S.). Ethical approval for this study was obtained from the Ethics Committee, Kagoshima City Hospital, and informed consent was obtained from all patients.

REFERENCES

1. Kelly NE, Wendel RT. Vitreous surgery for idiopathic macular holes. Results of a pilot study. Arch Ophthalmol 1991;109(5):654–659.
2. Brooks HL Jr. Macular hole surgery with and without internal limiting membrane peeling. Ophthalmology 2000; 107(10):1939–1948.
3. Park DW, Sipperley JO, Sneed SR, Dugel PU, Jacobsen J. Macular hole surgery with internal-limiting membrane peeling and intravitreous air. Ophthalmology 1999;106(7):1392–1397.
4. Margherio RR, Margherio AR, Williams GA, Chow DR, Banach MJ. Effect of perifoveal tissue dissection in the management of acute idiopathic full-thickness macular holes. Arch Ophthalmol 2000;118(4):495–498.
5. Kitaya N, Hikichi T, Kagokawa H, Takamiya A, Takahashi A, Yoshida A. Irregularity of photoreceptor layer after successful macular hole surgery prevents visual acuity improvement. Am J Ophthalmol 2004;138(2):308–310.
6. Villate N, Lee JE, Venkatraman A, Smiddy WE. Photoreceptor layer features in eyes with closed macular holes: optical coherence tomography findings and correlation with visual outcomes. Am J Ophthalmol 2005;139(2):280–289.
7. Baba T, Yamamoto S, Arai M, et al. Correlation of visual recovery and presence of photoreceptor inner/outer segment junction in optical coherence images after successful macular hole repair. Retina 2008;28(3):453–458.
8. Chang LK, Koizumi H, Spaide RF. Disruption of the photoreceptor inner segment–outer segment junction in eyes with macular holes. Retina 2008;28(7):969–975.
9. Sano M, Shimoda Y, Hashimoto H, Kishi S. Restored photoreceptor outer segment and visual recovery after macular hole closure. Am J Ophthalmol 2009;147(2):313–318.
10. Michalewska Z, Michalewski J, Cisiecki S, Adelman R, Nawrocki J. Correlation between foveal structure and visual outcome following macular hole surgery: a spectral optical coherence tomography study. Graefes Arch Clin Exp Ophthalmol 2008;246(6):823–830.
11. Inoue M, Watanabe Y, Arakawa A, Sato S, Kobayashi S, Kadonosono K. Spectral-domain optical coherence tomography images of inner/outer segment junctions and macular hole surgery outcomes. Graefes Arch Clin Exp Ophthalmol 2009;247(3):325–330.
12. Takahashi H, Kishi S. Tomographic features of early macular hole closure after vitreous surgery. Am J Ophthalmol 2000; 130(2):192–196.
13. Ko TH, Fujimoto JG, Duker JS, et al. Comparison of ultrahigh- and standard-resolution optical coherence tomography for imaging macular hole pathology and repair. Ophthalmology 2004;111(11):2033–2043.
14. Ko TH, Witkin AJ, Fujimoto JG, et al. Ultrahigh-resolution optical coherence tomography of surgically closed macular holes. Arch Ophthalmol 2006;124(6):827–836.
15. Moshfeghi AA, Flynn HW, Elner SG, Puliafito CA, Gass JDM. Persistent outer retinal defect after successful macular hole repair. Am J Ophthalmol 2005;139(1):183–184.
16. Privat E, Tadayoni R, Gaucher D, Haouchine B, Massin P, Gaudric A. Residual defect in the foveal photoreceptor layer defected by optical coherence tomography in the eyes with spontaneously closed macular holes. Am J Ophthalmol 2007;143(5):814–819.
17. Christensen UC, Krøyer K, Sander B, Larsen M, la Cour M. Prognostic significance of delayed structural recovery after macular hole surgery. Ophthalmology 2009;116(12):2430–2436.